Release and co-release of model hydrophobic and hydrophilic actives from 3D printed kappa-carrageenan emulsion gels

Kamlow, Michael-Alex; Holt, Thomas; Spyropoulos, Fotios; Mills, Tom

DOI:
10.1016/j.foodhyd.2022.107852

Document Version
Peer reviewed version

Citation for published version (Harvard):
Kamlow, M-A, Holt, T, Spyropoulos, F & Mills, T 2022, 'Release and co-release of model hydrophobic and hydrophilic actives from 3D printed kappa-carrageenan emulsion gels', *Food Hydrocolloids*, vol. 132, 107852. https://doi.org/10.1016/j.foodhyd.2022.107852

Release and co-release of model hydrophobic and hydrophilic actives from 3D printed kappa-carrageenan emulsion gels

Michael-Alex Kamlow, Thomas Holt, Fotis Spyropoulos, Tom Mills

School of Chemical Engineering, University of Birmingham, Edgbaston, Birmingham, B15 2TT, United Kingdom

Abstract

This study formulated and compared 3D printed (3DP) and cast kappa-carrageenan (κC) emulsion gels for the co-release of model lipophilic (cinnamaldehyde) and hydrophilic (erioglaucine disodium salt (EDS)) molecules. Tween 20 (T20) or whey protein isolate (WPI) were used as the emulsifier. Both 3DP and cast emulsion gels maintained their oil droplet size over 8 weeks owing to the set gel matrix. Penetration texture analysis revealed 3DP and cast 5% oil emulsion gels, required more force to break compared to 40% oil gels (3 N against 0.4-0.5 N). This was because the oil droplets, disrupted the gel matrix; thereby weakening it. 3DP gels required less force to break than cast gels, owing to failure between the printed layers. Release tests in various media showed no significant difference in the final % cinnamaldehyde released between 3DP gels and cast gels. Release tests in carried out 0.1M hydrochloric acid saw an increase in cinnamaldehyde release compared to other media, owing to cinnamaldehyde's increased solubility in acidic media. Addition of EDS into the gel matrix facilitated co-release studies, with EDS release having no effect on the cinnamaldehyde release, indicating EDS release was driven by liberation from the gel network and cinnamaldehyde release by its expulsion from the oil droplets. Simple modelling showed that diffusion rather than polymeric relaxation was more dominant for active release in 3DP gels compared to cast gels. This work shows that 3DP can be used to produce customisable κC-emulsion gels, with multiple actives; suitable for use as modified release vehicles.

1. Introduction

3D-printing (3DP), otherwise known as additive manufacturing, is a production technique that uses digital files rendered slice by slice to create products in a layer-by-layer manner. Initially 3DP was primarily concerned with construction materials such as plastic polymers (Rahim, Abdullah, & Md Akil, 2019), ceramics (Z. Chen, et al., 2019) and metals (Buchanan & Gardner, 2019). However, 3DP research has expanded to encompass various other research avenues including pharmaceuticals (Goyanes, et al., 2017), and edible ingredients such as dough (Fan Yang, Zhang, Prakash, & Liu, 2018), dairy gels (Daffner, Ong, Hanssen, Gras, & Mills, 2021; Daffner, Vadodaria, et al., 2021), chocolate (Lanaro, Desselle, & Woodruff, 2019) and many more, via a variety of methods (Gholamipour-Shirazi, Kamlow, T Norton, & Mills, 2020). 3DP of food is an area of much research interest owing to its ability to create highly customisable products at the point of consumption or sale, and make alterations without the need for moulding or tooling (Sun, et al., 2015). As things stand, there still exist process disadvantages compared to current mass production techniques, including high cost per individual item, low-throughput and a restricted repertoire of printable edible materials; which still require further research (Pallottino, et al., 2016).

One of the major issues within the area of food 3DP is undoubtedly the multifaceted nature of food systems, comprising multiple phases in varying ratios, micro- and nanostructure factors that affect structural and sensory traits and sensitivity to processing, ion and temperature changes (Ubbink, Burbidge, & Mezzenga, 2008). Hydrocolloid gels (hereafter referred to as hydrogels) have become an area of much interest within the field of 3DP. Hydrogel formulations commonly consist of 0.1-10% w/w hydrocolloid, small quantities of salts and water. Therefore, there is much scope for flexible formulations using hydrogels as a starting base. This can involve the addition of sugars, salts and other hydrophilic molecules (Ricci, Derossi, & Severini, 2019). Past 3DP studies into hydrogels have focused on agar (Serizawa, et al., 2014), starch (Huan Chen, Xie, Chen, & Zheng, 2019), alginate (Jin, Compaan, Bhattacharjee, & Huang, 2016) and mixtures of materials (Fenton, Gholamipour-Shirazi, Daffner, Mills, & Pelan, 2021; Z. Liu, Bhandari, Prakash, Mantihal, & Zhang, 2019; Vadodaria, He, Mills, & Wildman, 2020)

One biopolymer of specific interest in hydrogel 3DP is kappa-carrageenan (κC). κC is an anionic, sulphated polysaccharide extracted from an edible seaweed named Rhodophyta. When dispersed in water, alongside complementary gelling cations, κC forms firm, thermally reversible gels. The most effective gelling cation for κC is potassium (Hermansson, Eriksson, & Jordansson, 1991). When the hot dispersion is lowered below its gelation temperature (T_{gel}), random κC coils order themselves into double helices, and these aggregate to form a polymeric network (Norton, Morris, & Rees, 1984). κC has been used as a hydrogel feed source for cold-extrusion 3DP (Gholamipour-Shirazi, Norton, & Mills, 2019), hot extrusion 3DP by itself (Diañez, et al., 2019), and as part of a mixed-system (Gholamipour-Shirazi, Norton, & Mills, 2021).

The need to produce more complex feeds for 3DP has turned attention to emulsion gels, involving the production of an oil-in-water (o/w) emulsion and then dispersing gelling agents within the water phase. These gels more closely resemble real food systems compared to simple water based hydrogels. This facilitates the production of more complex and customisable products and enables the straightforward incorporation of lipophilic molecules. Since 3DP has the potential to customise food assemblies through precise ingredient placement and distribution, emulsion gels are ideal candidates for further study. Their uses include modification of food texture (Matsumura, Kang, Sakamoto, Motoki, & Mori, 1993) and delivery of lipophilic molecules both alone (F. Liu & Tang, 2016; Thakur, et al., 2012; Zhang, et al., 2022) and alongside hydrophiles (Singla, Saini, Joshi, & Rana, 2012). There has been some study into 3DP of emulsion gels (Hu, et al., 2019; Johannesson, Khan, Hubert, Teleki, & Bergström, 2021; Wang, et al., 2021), but as far as the authors are aware none involving κC-emulsion gels apart from a previous study (Kamlow, Spyropoulos, & Mills, 2021). There is currently an increasing interest in the formulation of multi-dose medicines and nutritionally fortified foods (David Julian McClements, 2018; Nagula & Wairkar, 2019). Therefore emulsion gels are an obvious area for research in the sphere of functional foods, owing to their biphasic nature, and ability to manipulate energy levels through oil content. However, despite this, none of the previous studies assessed the release of a model lipophile (cinnamaldehyde) with and without a model hydrophile (Erioglaucine disodium salt) compared to the cast equivalent. Even though previous studies have shown that by moving from cast to 3DP bulk structures, you can affect a change in release rates, while providing a far greater degree in flexibility with respect to dosage size, shape and appearance (Kamlow, Vadodaria, Gholamipour-Shirazi, Spyropoulos, & Mills, 2021).

Cinnamaldehyde is an essential oil extracted from the bark of cinnamon trees. It has antibacterial and antifungal properties (Gill & Holley, 2004; Siddiqua, Anusha, Ashwini, & Negi, 2015) as well as antioxidant activity (Gowder & Devaraj, 2006). Cinnamaldehyde has a log P

of 1.82, meaning that it has very limited water solubility, but retains enough to be able to track the release over time from a lipophilic environment to a hydrophilic one (Ben Arfa, Preziosi-Belloy, Chalier, & Gontard, 2007). Cinnamaldehyde has been utilised in release studies before, and is an optimal model lipophile owing to its ability to partition from an oil phase into a water phase, pleasant aroma and safety profile, being generally recognised as safe by the food and drug administration (Govindaraj, Subramanian, & Raghavachari, 2021). Erioglaucine disodium salt (EDS) is a water-soluble dye that once dissolved gives a blue colour and is often used in release studies as a model hydrophilic molecule (Andrews, et al., 2009; Jeong, et al., 2021; Lu, Tarn, Pamme, & Georgiou, 2018).

The present study aims to evaluate the release of model lipophilic with and without hydrophilic small molecular weight species from hot extrusion 3DP κC-emulsion gels, and assess their performance compared to the equivalent cast gels, in order to assess the performance of both as possible solid dosage forms or implants. This involved formulating 3% w/w κC-emulsion gels containing either 5% or 40% w/w sunflower oil (SFO) and stabilised with Tween 20 (T20) or whey protein isolate (WPI). After production of simple o/w emulsions with and without cinnamaldehyde, with a monomodal or bimodal distribution, droplet size was tested through dynamic light scattering and emulsion stability was scrutinised via zeta-potential measurements. κC-emulsion solutions were created by dispersing κC powder into the simple emulsions while heating. Following this, κC-emulsion gels were created either by 3DP or casting in moulds. 3DP and cast κC-emulsion gels had their stability tested through droplet size measurements utilising time domain nuclear magnetic resonance (NMR) spectroscopy and through syneresis measurements. The gels' mechanical properties were also scrutinised through texture profile analysis, namely penetration tests, comparing 3DP and cast gels. Finally, the printed and cast gels underwent release tests to assess their performance as release vehicles in various release media, with cinnamaldehyde release examined. After this EDS was loaded into the gels as a model molecule to test hydrophilic release and co-release studies were carried out.

2. Materials and methods

2.1. Materials

κC, T20, cinnamaldehyde, potassium chloride (KCl), and EDS were purchased from Sigma-Aldrich (UK). High performance liquid chromatography grade pentane and 32% w/v HCl were purchased from Honeywell, (UK). Phosphate Buffer Solution (PBS) tablets were obtained from Oxoid (UK). WPI was obtained from Sachsenmilch Milk & Whey Ingredients (Sachsenmilch Leppersdorf GmbH, Wachau, Germany). According to the manufacturer it contained 93.74% w/w protein in dry matter, 0.23% w/w fat, 0.61% w/w lactose and 3.16% w/w ash. SFO was purchased from the supermarket Spar (UK). Milli-Q water was used (Elix® 5 distillation apparatus, Millipore®, USA) for sample preparation. All materials were used as received with no further modification or purification.

2.2. Emulsion preparation

Simple emulsions containing no κC were produced for particle size analysis before gelation and zeta-potential measurements. Production of the emulsions followed the same procedure as that previously described by (Kamlow, Spyropoulos, et al., 2021). Emulsions stabilised with T20 had 1% w/w T20 added to the required amount of water and SFO. Emulsions stabilised with WPI had a 2% w/w stock solution of WPI diluted to 1% w/w WPI by adding deionised water and SFO. These mixtures where then premixed on a Silverson L5M for 3 minutes at

6000 rpm with a fine emulsor screen. The formed pre-emulsions were then passed through a high-pressure homogeniser at 25 bar to produce smaller scale emulsions with a droplet size of approximately 1 μm and 1000 bar to produce larger-scale emulsions with a droplet size of approximately 8-18 μm. Emulsions containing cinnamaldehyde had 0.7% w/w of the SFO fraction replaced with cinnamaldehyde and these were stirred together using a magnetic stirrer for ten minutes to ensure complete mixing. To create bimodal droplet size distribution emulsions, larger and smaller scale emulsions were created and then mixed 50/50 by stirring with a magnetic stirrer for five minutes.

2.3. κC-Emulsion solution preparation

T20 and WPI stabilised O/W emulsions (as described in section 2.2) with and without cinnamaldehyde were used for the preparation of κC-emulsion solutions as described by (Kamlow, Spyropoulos, et al., 2021). Emulsions were heated for 30 minutes on a hot-plate stirrer set to 80 °C. Then κC was added and left to stir for two hours to ensure that all κC had dispersed. 3% w/w κC in the water phase was chosen as this has been reported to give optimal printing outcomes (Kamlow, Spyropoulos, et al., 2021; Kamlow, Vadodaria, et al., 2021). Finally, O/W emulsion gels were formed by cooling the systems, either via 3D printing as described in section 2.8 or casting in moulds as described in section 2.9.

2.4. κC-EDS-emulsion solution preparation

For the co-release tests, κC-emulsion solutions containing EDS were prepared to test the release of EDS by itself. Emulsions were produced as in section 2.3, but with 7.04g of water removed. Then after κC-emulsion production, 7.04g of EDS 2% w/w solution was added to the hot κC-emulsion solution and stirred for a further 30 minutes. This solution could then be gelled via 3D printing as in section 2.8 or casting in moulds as in section 2.9.

2.5. κC-EDS-emulsion with cinnamaldehyde solution preparation

For the co-release tests, κC-EDS-emulsion solutions containing cinnamaldehyde were produced by following the method in 2.4 but utilising an emulsion that had 0.7% w/w of the SFO fraction replaced with cinnamaldehyde.

2.6. Simple emulsion droplet size analysis

The emulsion droplet size was obtained using a Malvern Mastersizer MS 2000, (Malvern Panalytical, UK), utilising a Hydro SM manual small volume sample dispersion unit. This gave data for Surface weighted mean ($D_{3,2}$) and volume weighted mean ($D_{4,3}$) droplet size values were obtained immediately after preparation. The values for refractive index were input into the software and were 1.33 for water and 1.467 for the sunflower oil. For the SFO mixed with cinnamaldehyde, a refractometer (J357 Automatic refractometer, Rudolph research) was used to calculate the refractive index of the mixture. Cinnamaldehyde was found to have a refractive index of 1.62, and the mixture of cinnamaldehyde and sunflower oil was found to be 1.468. Samples were dispersed in distilled water at 1300 rpm to give an obscuration value of 4.2-4.6%. Samples were prepared and tested in triplicate and droplet size values were the average of at least three measurements.

2.7. Zeta-potential measurement

The zeta potential (ζ-potential) was determined using a Zetasizer (Malvern Panalytical, UK) in order to assess the stability of the emulsions created and to assess if replacing part of the SFO fraction with cinnamaldehyde affected stability. Samples were diluted 100 times with deionised water (Wu, et al., 2016). This was to reduce the absorbance of laser light and multiple scattering. All ζ-potential measurements were carried out at room temperature.

2.8. 3D printing

The 3D printer was supplied by the Institute of Food Science and Biotechnology at the University of Hohenheim (Germany). It is a Fabbster 3D printer that was modified in order to handle a liquid feed. Full detail of the printer's setup and function can be found in a previous study (Kamlow, Spyropoulos, et al., 2021). After production of κC-emulsion solutions as in sections 2.3-2.5, these were fed into the printer, with the temperature being maintained indirectly via double walled pipes containing heated water in counterflow. The syringe was also wrapped in a heated jacket to prevent pre-gelation. The computer would then slice the desired 3D printed shape into layers and send this information to the printer which would then move in the X, Y and Z axes to produce the 3D shape. The material flowed via a syringe driver with a controllable flow rate, which was important as 5% w/w SFO and 40% w/w SFO emulsion solutions had different viscosities, necessitating two different flow rates (Pal & Rhodes, 1989).

The printing parameters for these emulsion gels were determined in a previous study (Kamlow, Spyropoulos, & Mills, 2021). The replacement of 0.7% of the SFO with cinnamaldehyde, as well as the addition of 0.1408% w/w EDS in the water phase had no effect on the printability of the gels which were printed at the optimal parameters previously defined. These were a printer bed temperature of 35 °C, print speed of 30 mm/s, fill space of 1.25 mm, a water bath temperature on the feed pipes of 72 °C, a water bath temperature on the nozzle of 72 °C, layer height of 1.2 mm, nozzle size of 20G/0.8mm and nozzle height of 0.5 mm. The syringe driver rate was 0.7 mL/min for 5% SFO κC-emulsion gels and 0.84 mL/min for 40% SFO κC-emulsion gels. This was used to produce 20 x 20 x 9 mm cuboids for texture profile analysis and syneresis testing, 15 x 15 x 30 mm cuboids for droplet size testing and 15mm height and 12 mm diameter cylinders for release tests. These are shown in Fig 1.

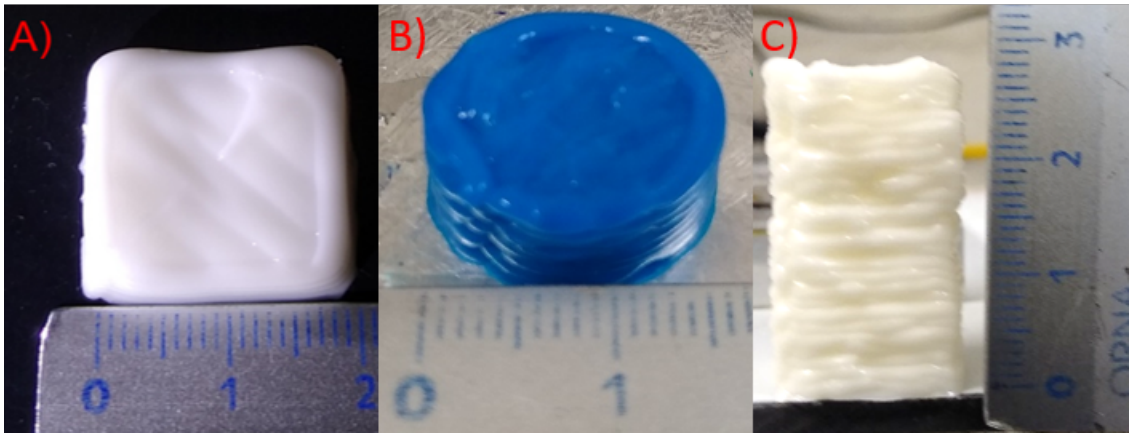

Figure 1: 3DP (A) 20 x 20 x 9.6 mm cuboid, (B) Cylinder containing EDS and (C) 15 x 15 x 30 mm cuboid

2.9. Production of moulds for casting

Cylinder and cuboid shaped moulds were produced using a form 2 stereolithography 3D printer (Formlabs, USA). The moulds were designed by computer aided design and uploaded to the software, digitally sliced into layers, then transmitted to the printer digitally to print. The cube mould facilitated the production of emulsion gel cuboids with dimensions of 20 x 20 x 9.6 mm by casting. These were then used for comparative penetration testing as a control, cast sample to compare to the 3D printed cuboids produced in 2.8. The cylinder mould was used to produce cast, control samples for release tests of cinnamaldehyde, EDS or both at the same time, to compare to the 3D printed cylinders produced in 2.8.

2.10. Syneresis testing

KC emulsion gel cuboids containing 5% or 40% SFO with dimensions of 20 x 20 x 9.6 mm were produced by 3D printing or casting and stored in an airtight container at 5 ˚C. Syneresis measurements were carried out by measuring the amount of water release by the emulsion gels after several time intervals as described in a previous study (Ako, 2015). The syneresis ratio (R_s) was determined using equation 1.

$$R_s = \frac{w_e}{w_g} x\ 100 \quad Eq\ [1]$$

Where w_e is the weight of water released by the gel, and w_g is the weight of the initial gel. Since 40% SFO emulsion gels contain considerably less water per 100g compared to 5% SFO emulsion gels, the values were normalised to a constant water concentration.

2.11. Time-Domain nuclear magnetic resonance spectroscopy

Droplet size measurements of the emulsion gels were performed using an NMR device (Bruker Minispec NMR, Bruker Optics, UK), equipped with a gradient unit. Measurements were performed on three different samples, in triplicate. Droplet size calculations were performed using the Minispec software, which fits the data to a log-normal curve. Measurements were taken to assess the stability of the emulsion gels over 8 weeks, with samples tested at 0, 1, 2, 3, 4 and 8 weeks. Cast gels were tested by adding hot κC-emulsion gel solution to the NMR tubes. 3DP gels were tested by printing a cuboid measuring 15 x 15 x 30 mm and then using a cork borer, the same size as the internal diameter (Ø 10mm) of the NMR tubes to cut out a cylinder and place that into the NMR tube. $D_{3,2}$ values from section 2.6 were converted to the volume-weighted geometric mean diameter ($D_{3,3}$) values to be used as a comparison to see if oil droplet sizes changed during gelation, using equation 2 insert reference on endnote - https://doi.org/10.1006/jcis.2001.7603.

$$D_{3,3} = \frac{D_{3,2}}{e^{-\sigma^2 \div 2}} \quad \text{Eq [2]}$$

where $D_{3,3}$ is the geometric weighted mean diameter, $D_{3,2}$ is the surface weighted mean diameter and σ is the standard deviation of the logarithm of the droplet diameter.

2.12. Texture Profile Analysis

Texture profile analysis (TPA) was carried out using a TA XT plus Texture Analyser. Printed and cast cuboids of dimensions 20 × 20 × 9.6 mm were tested; the cast cuboids were given 3 minutes 30 seconds to set, mimicking the time taken to print their respective counterparts. Penetration testing was carried out using a P/6 cylindrical aluminium probe set to a constant speed of 0.5 mm/s, over a distance of 6 mm, alongside a 30 kg load cell and 3 g of trigger force. Through penetration testing, data for the force at breaking, firmness and gel strength were acquired for printed and cast cuboids. Force at breaking, in g, is defined as the first significant discontinuity produced in the curve during penetration (Fiszman, Lluch, & Salvador, 1999). Firmness, in g/mm, is the initial slope of the penetration curve within the first 2 seconds (Fiszman & Salvador, 1999). Gel strength, in g x mm, is the multiplication of the penetration force by the distance of the penetration where failure occurs (H. Liu, Nie, & Chen, 2014). All tests were carried out in triplicate.

2.13 Release studies

Release studies were carried out using ultraviolet (UV)-visible spectrophotometry to assess the release of cinnamaldehyde from the printed and cast κC-emulsion gels. All studied gel systems were of a consistent weight; 1700 mg ± 5%. Oil droplets were tested at both the micron and sub-micron scale. Three cast and three printed κC-emulsion gels were each placed inside semipermeable cellulose dialysis membrane (approx. 80 mm x 40 mm), which had been

soaked for 24 hours in deionised water. The molecular weight cut-off for the membrane was stated to be 14,000 Daltons. This was far below the molecular weight of the κC, ensuring none would interfere with the absorbance readings (Phillips & Williams, 2009). The gel-containing membranes were placed within 150 mL of various media (deionised water, PBS, 0.1 M HCl and 1 M KCl). 100% release of the cinnamaldehyde within the gels would equate to approximately 4 mg/L. Since this is significantly lower than the maximum solubility within water, this equates to sink conditions. The release tests were carried out within an Incu-Shake MIDI shaker incubator (Sciquip, UK) at 150 rpm. Release tests were carried out at 37 ˚C for *in vitro* testing. Measurements were taken at various time points up to and including 360 minutes. Determination of the cinnamaldehyde release was carried out using a Jenway Genova Bio life science spectrophotometer (Cole-Parmer, UK), set to 290 nm, the maximum absorbance for cinnamaldehyde in the various release media. 0.9 mL of dissolution medium was taken with an Eppendorf pipette and tested at the times stated above. This was placed into the UV-Vis spectrophotometer which had been blanked using fresh release media. The release profile was calculated from a calibration curve determined by the UV-Vis spectrophotometer, which had an R^2 value of 0.999. The contents of the cuvette were then discarded and 0.9 mL of fresh medium added into each beaker. This was corrected when determining the cinnamaldehyde release percentage following the procedure of (B. Singh, Kaur, & Singh, 1997). All tests were carried out in triplicate.

2.14 Co-release studies

Co-release studies were carried out in water using a modified version of the protocol in 2.13. KC-EDS-emulsion gels with cinnamaldehyde were cast and printed, placed within semipermeable cellulose dialysis membrane, then placed into beakers containing 150 mL water. 100% release of the EDS would equate to approximately 8 mg/L, which meant that it was being released into sink conditions. 1.8 mL aliquots were taken at the various release points. 0.9 mL was taken and tested for EDS release at 629 nm on the UV-vis spectrophotometer, which had been blanked against deionised water. The release profile was calculated from a calibration curve for the EDS which had an R^2 value of 0.999. Then a solvent extraction protocol was carried out on the remaining 0.9 mL. 0.9 mL of pentane was added to the remaining 0.9 mL of the aliquot and they were shaken together. The cinnamaldehyde was far more soluble in the pentane than the water, but the EDS is insoluble in the pentane (Balaguer, et al., 2013). This prevented any interference from the EDS when measuring the absorbance of the cinnamaldehyde in the pentane. This was tested within the UV-vis spectrophotometer at 280 nm, as being within pentane caused a shift in the maximum absorbance peak compared to being dissolved within water. Blank pentane that had been shaken through deionised water was used to blank the instrument. A separate calibration curve was created for cinnamaldehyde in pentane which had an R^2 value of 0.990.

2.15 Modelling of release data

Cinnamaldehyde and EDS release data (up to 60%) were fitted to the following model (Ritger & Peppas, 1987)

$$\frac{M_t}{M_\infty} = k_1 t^m + k_2 t^{2m} \qquad \text{Eq [3]}$$

where $Mt / M\infty$ is the fraction of active released at time t. The first term ($k_1 t^m$) relates to Fickian effects while the second term ($k_2 t^{2m}$) to relaxational contributions to the release. k_1 is the kinetic constant regarding release from the matrix by Fickian diffusion and $k2$ is the kinetic constant for case-II relaxation. Lastly the coefficient m is the purely Fickian diffusion exponent which is dependent on the shape of the device; the value of the exponent concerning relaxation transport is in theory twice the Fickian exponent ($2m$). This modelling yielded values between 0.5 and 1. The closer to 0.5, the greater the contribution of Fickian diffusion to the release of the molecules. The closer to 1.0, the greater the contribution of polymeric relaxation to molecular release.

2.16 Statistics

The average droplet size, ζ-potential, R_s, force at break, gel strength, firmness and cumulative release % were compared using the two-sample T-test in the Analysis ToolPack for Microsoft Excel. Confidence levels were set at 95%. Therefore, if $P < 0.05$, the two sets of data have different means, otherwise the two means have no significant statistical difference.

3. Results and discussion

3.1. Droplet size analysis and zeta-potential measurements

The o/w emulsions containing 5% or 40% w/w SFO (dispersed phase) and stabilised by either T20 or WPI, were studied both in the presence and absence of included cinnamaldehyde; comprising 0.7% of the total oil fraction in each system. Emulsifier concentration was fixed at 1% w/w, which was sufficient to stabilise the emulsions. It was important to characterise the simple emulsions before conversion to emulsion gels, for printing, in order to establish a baseline for later stability testing (see section 3.3). These systems were all formed in dimensions that were able to undergo printing through the 0.8 mm nozzle, practically undisturbed. They were also determined to be stable during the heating step described in section 2.3, and thus are not expected to change from production to printing. We were able to deliver systems with controlled variations to droplet length scale, emulsifier type, dispersed phase content as well as droplet surface charge. Establishment of this level of customisation is important for proving the use of 3DP κC-emulsion gels as flexible delivery systems for targeted molecules. $D_{4,3}$ droplet size data is presented in Fig. 2A for larger scale and Fig 2B for smaller scale emulsions.

Statistical analysis showed no significant difference in the droplet sizes produced by varying the SFO concentration or by replacing 0.7% of the oil fraction with cinnamaldehyde, in either length scale. However, there is a statistically significant difference between the emulsions stabilised by T20 compared to those stabilised by WPI. This is due to T20 being a low molecular weight surfactant (LMWS), meaning it can position itself faster at the interface (Kenta, et al., 2013). Furthermore, LMWS are superior at decreasing the water/oil interfacial tension compared to proteins, further aiding droplet breakup (Beverung, Radke, & Blanch, 1999).

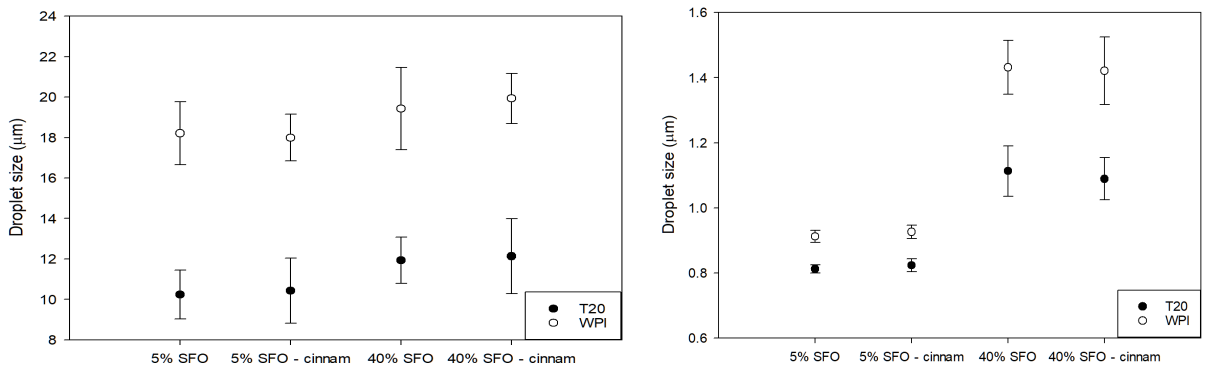

Figure 2: Comparison of the average droplet size of emulsions with and without cinnamaldehyde containing 5% or 40% SFO and 1% w/w T20 or WPI in the larger (A) or smaller (B) scale.

Bimodal distributions were also created to be used for stability testing (see section 3.3), with larger and smaller scale emulsions mixed in a 1:1 ratio. Because release studies were to be carried out, the possibility of custom release profiles created by mixing different droplet sizes in varying ratios, meant that purpose made bimodal droplet distributions were investigated as well. However, since the $D_{4,3}$ values from the mastersizer are calculated for monomodal distributions, it is far more practical to show the droplet distribution graphs, which are given in Fig 3, including the distributions of the individual size scale systems. This is because a single, average droplet size value does not fully represent the equally mixed droplet populations for the mixed size scale systems.

The distributions in Fig. 3 showed that there was no significant difference when replacing 0.7% of the oil fraction with cinnamaldehyde. Furthermore, the mixing of the larger and smaller scale emulsions created bimodal distributions, which reflected the two constituent monomodal distributions of which they were comprised.

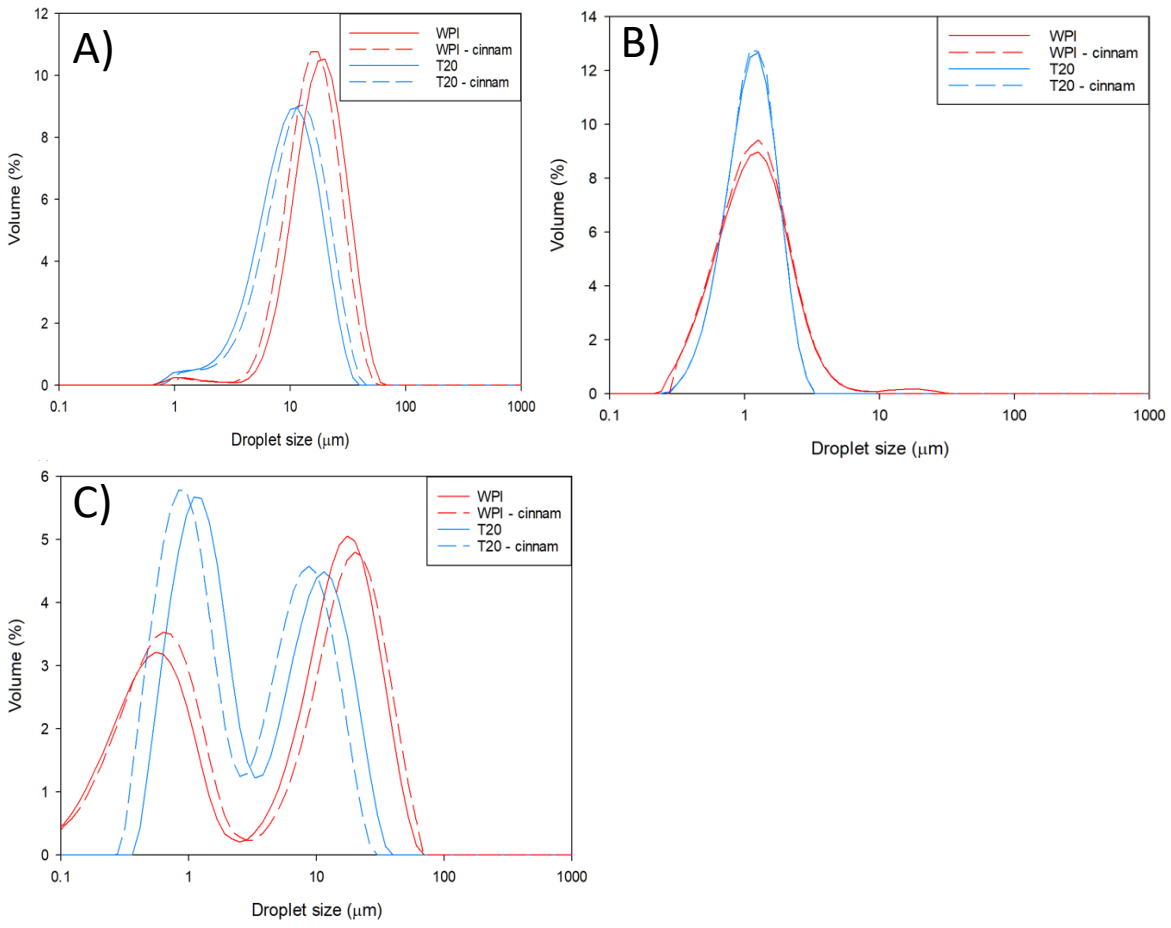

Figure 3: $D_{4,3}$ distribution of 40% SFO (A) larger scale emulsions, (B) smaller scale emulsions and (C) mixed scale emulsion systems stabilised with either T20 or WPI.

The emulsions were also tested for their ζ-potential, to assess whether the different emulsifiers, the changes in length-scale of the emulsion droplets, or the addition of the cinnamaldehyde fraction has an effect on surface charge (Fig 4). The ζ-potential values for T20 reflect that it is a non-ionic surfactant, which stabilises emulsions through steric repulsion, rather than surface charge (Teo, et al., 2016). The WPI stabilised emulsions had a strong

negative charge, owing to being above their isoelectric point, giving a ζ-potential value of around -34 mV to -37mV for larger-scale emulsions and a statistically significant difference of -29mV to -32 mV for the smaller-scale emulsions. This is fairly typical with smaller droplet sizes having been shown to present with a lower ζ-potential value (A. Wiącek & Chibowski, 1999; A. E. Wiącek & Chibowski, 2002). Replacing 0.7% of the SFO fraction with cinnamaldehyde did not have a statistically significant difference on the ζ-potential of the emulsions.

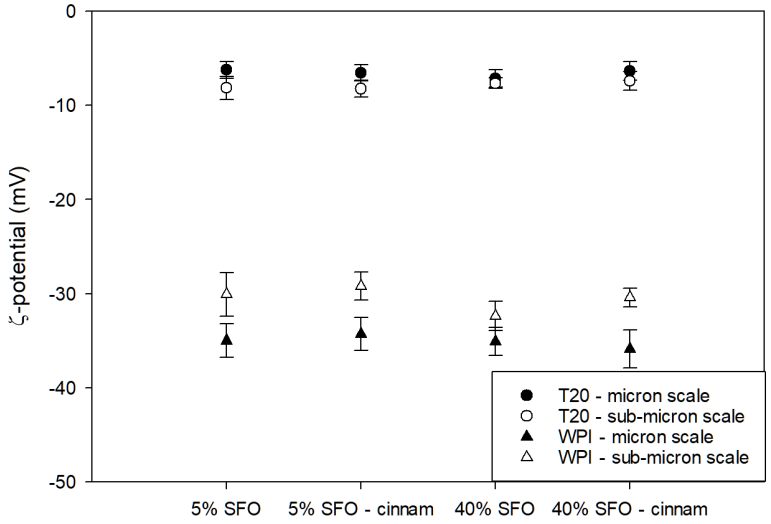

Figure 4: ζ-potential of O/W emulsions with and without cinnamaldehyde, stabilised by either T20 or WPI in the micron and sub-micron scale

3.2.Syneresis testing

During emulsion gel formation, while most water is retained within the gel network overtime, some is expelled during contraction over time as the polymer helices aggregate further (Thrimawithana, Young, Dunstan, & Alany, 2010). Syneresis is considered to be unfavourable when it comes to the use of biopolymer gels as molecular delivery vehicles, as any loss of water could lower the availability of any hydrophilic molecules within the water phase of the gels. Fig. 5 shows the results of syneresis testing over 28 days for cast and 3DP κC-emulsion gel cuboids containing 5% or 40% SFO stabilised by either T20 or WPI. The values have been normalised for the total water content.

As the gels continued to contract over time, water is expelled from within the gel matrix. The syneresis of the emulsion gels followed the same pattern, regardless of whether they were stabilised by T20 or WPI. Previous studies have shown that an increase in SFO concentration within emulsion gels reduces the water loss from syneresis; however, this study did not fix the biopolymer concentration to the water content (Hongqiang Chen, Lu, Yuan, Gao, & Mao, 2021). Therefore as the oil fraction increased, there was an effective increase of the biopolymer concentration within the aqueous phase of the emulsion gels. Furthermore while the data presented in Fig. 5 went to 40% w/w SFO, the previous study only assessed emulsion gels up to 20% SFO, making comparisons more difficult with previous reported results in literature. Here, there was no statistically significant difference between 5% and 40% SFO κC-emulsion in terms of water loss before 28 days had passed, then a statically significant difference was observed. One explanation for this could be the far higher oil concentration within the 40% SFO emulsion gels, causing greater disruption the network structure, leading

to a decrease in gel elasticity (D. Julian Mcclements, Monahan, & Kinsella, 1993). A decrease in elasticity of κC-emulsion gels has been shown to increase the rate of syneresis (Rostami, Nikoo, Rajabzadeh, Niknia, & Salehi, 2018). The authors have previously reported that 40% SFO κC-emulsion gels have lower elasticity compared to 5% SFO κC-emulsion gels (Kamlow, Spyropoulos, et al., 2021). The 3DP κC-emulsion gels lost more water than their cast equivalents, and this was believed to be due to the layering that runs through the 3DP κC-emulsion gels, as a consequence of the 3DP process, which can allow water a shorter route to exit the gels (Kamlow, Vadodaria, et al., 2021).

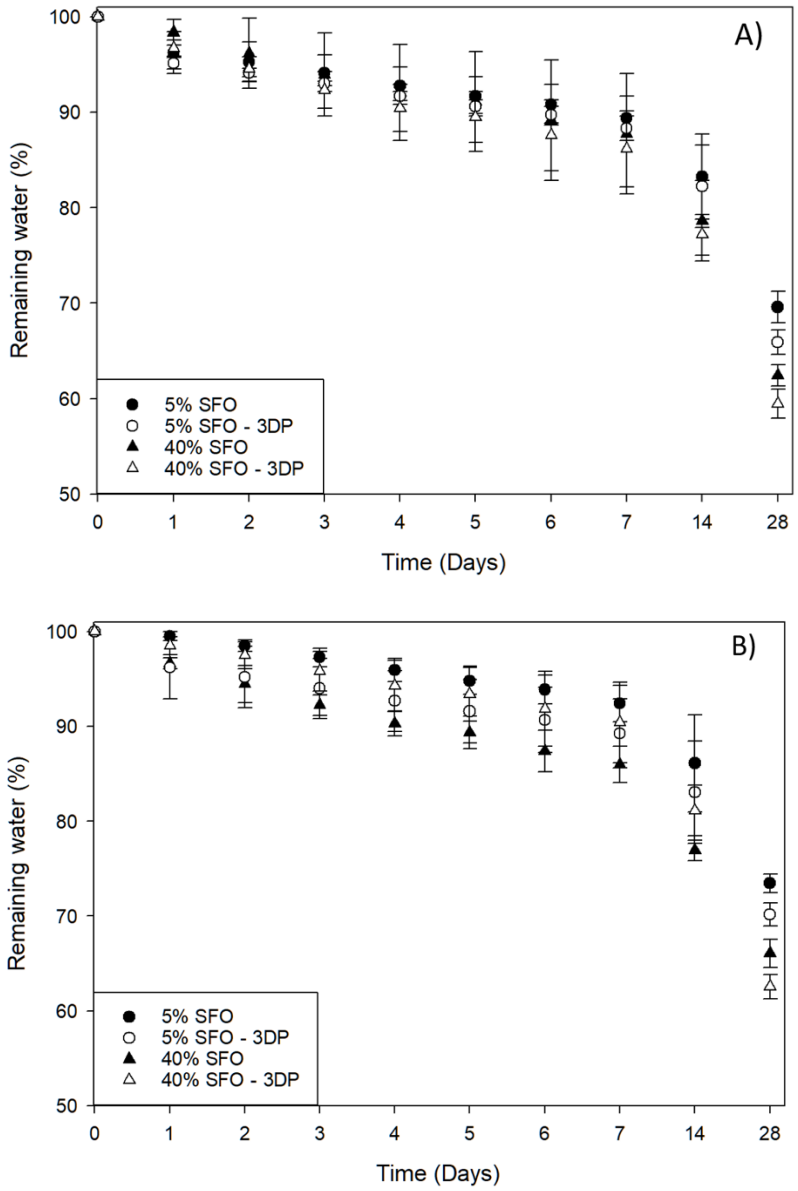

Figure 5: Syneresis of the κC-emulsion gels with different oil fractions for 3DP and cast κC-emulsion gels stabilised by (A) T20 and (B) WPI

3.3. Time Domain-NMR stability testing

Time Domain-NMR (TD-NMR) was used to evaluate the droplet size within κC-emulsion gel samples containing monomodal and bimodal droplet distribution systems in both the micron

and sub-micron scale. This was to assess whether the 3DP process, causes aggregation or flocculation of the emulsion systems, once gelled. TD-NMR has the advantage of being able to evaluate droplet size distributions within solid systems, unlike dynamic light scattering techniques and without the time-consuming nature of microscopy. Fig 6. Shows the data for emulsion gels over 8 weeks for micron and sub-micron, monomodally distributed κC-emulsion gel samples.

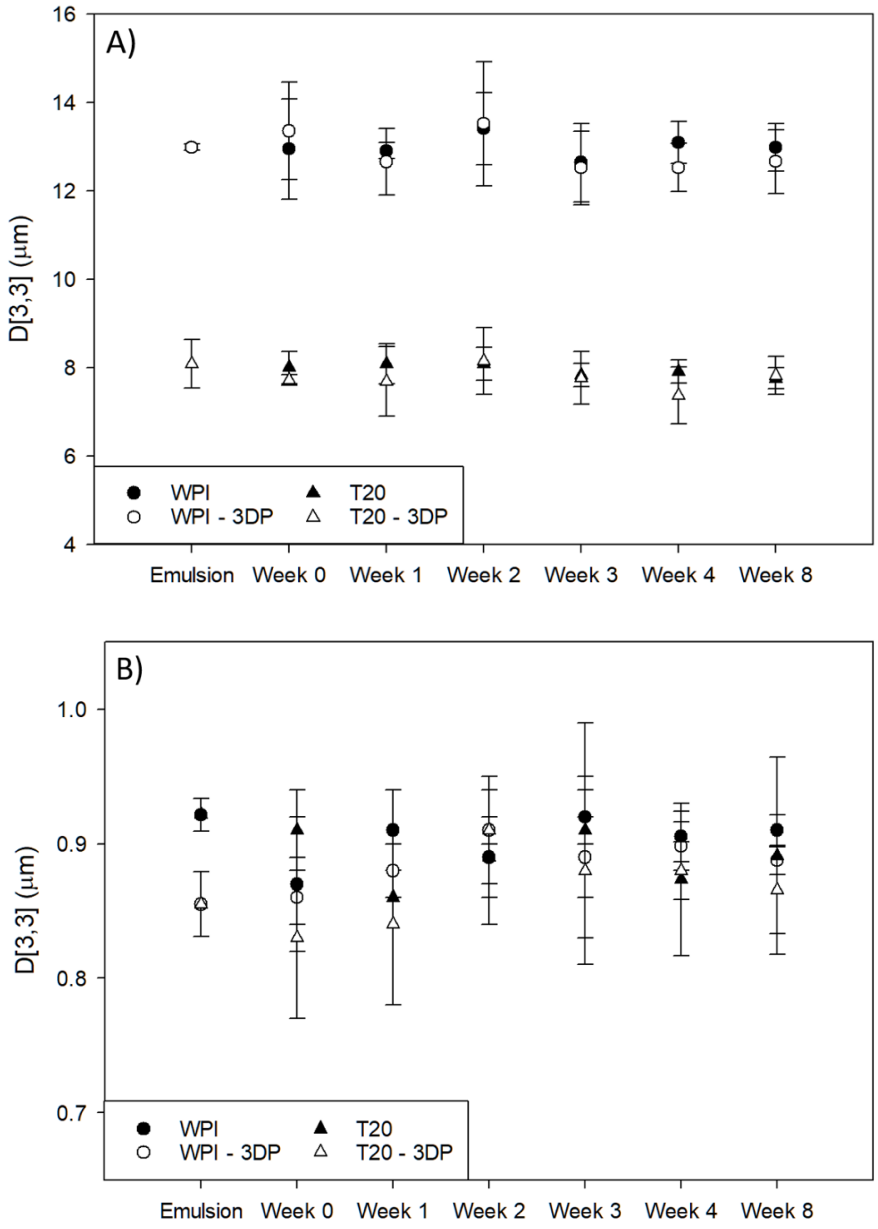

Figure 6: TD-NMR over 8 weeks showing $D_{3,3}$ values for cast and 3DP κC-emulsion gels in the micron (A) and sub-micron (B) scales

Fig. 6 showed that despite the simple emulsions being heated and stirred for two and a half hours during emulsion gel production, there was no significant coalescence of the oil droplets observed. Furthermore, the 3D printing process also appeared to have no significant effect on the oil droplet size within the κC-emulsion gels. The differences observed between the T20

and the WPI follow trends observed from section 3.1. While the droplet sizes appear to have stayed constant for both emulsifiers, the nature of TD-NMR means that it does not detect flocculation of oil droplets, as the restriction of self-diffusion of oil by the walls of the droplets, won't be affected by the flocculation (Goudappel, van Duynhoven, & Mooren, 2001). However, previous studies have shown that κC-emulsion gels flocculate when stabilised by T20 (Kamlow, Spyropoulos, et al., 2021; H. Singh, Tamehana, Hemar, & Munro, 2003). This doesn't occur with the WPI stabilised κC-emulsion gels, and is linked to the higher surface charge on the oil droplets stabilised by WPI (see Fig. 4). This highlights the need to examine complex systems such as emulsion gels through various techniques. There was no change seen over 8 weeks, which is due to the solid continuous phase restricting any movement of the oil droplets within the network.

Separately sub-micron and micron scale emulsions were created and mixed by stirring for five minutes and then gelled as above. These were also stored for 8 weeks and the droplet sizes examined. Fig. S1 and table 1 show that despite intentionally creating a bimodal emulsion distribution, the emulsion gels maintained their stability over 8 weeks. This is despite the fact that bimodal emulsions are less stable, and more prone to Ostwald ripening and coalescence (van der Ven, Gruppen, de Bont, & Voragen, 2001). The addition of cinnamaldehyde caused no significant change to the droplet sizes. Since $D_{3,3}$ are calculated based on monomodal distributions, these values alone are not fully representative of the droplet size distributions present within these systems (Juslin, Antikainen, Merkku, & Yliruusi, 1995). It also appears that the tween emulsion gel systems appear to have eliminated the flocculation observed in the simple emulsion systems. The distribution values over 8 weeks are presented in table 1.

Table 1 shows that the emulsion gels for the mixed-scale systems maintained the same distributions and σ values after production and storage for 8 weeks. The σ value corresponds to the standard deviation of the logarithm of the droplet diameter. The κC-emulsion gels stabilised with T20 had a narrower droplet size distribution owing compared to those stabilised by WPI, which is reflected in the smaller σ value. The demonstrated ability of emulsion gels to maintain emulsion stability over time, coupled with their thermoreversible nature means that they could potentially be used to store poorly stable emulsions as emulsion gels, and then heat them to undergo a gel-sol transition and consume them as a liquid form if needed.

Table 1: Data on droplet size distributions of mixed scale κC-emulsion gels following production and after 8 weeks. A higher σ value indicates a wider droplet size distribution

	Droplet size after 0 weeks				Droplet size after 8 weeks			
	WPI	T20	WPI with cinnamaldehyde	T20 with cinnamal dehyde	WPI	T20	WPI with cinnamal dehyde	T20 with cinnamal dehyde
Diameter 2.5% (μm)	0.31 ± 0.05	0.25 ± 0.04	0.30 ± 0.04	0.23 ± 0.02	0.28 ± 0.07	0.25 ± 0.02	0.24 ± 0.05	0.24 ± 0.01
Diameter 50% (μm)	5.80 ± 0.23	2.89 ± 0.15	5.79 ± 0.30	3.03 ± 0.09	5.83 ± 0.33	2.96 ± 0.02	5.72 ± 0.40	3.00 ± 0.04
Diameter 97.5% (μm)	81.88 ± 4.21	47.27 ± 2.23	77.61 ± 2.14	47.66 ± 3.19	79.37 ± 3.86	48.46 ± 1.69	77.45 ± 3.61	46.34 ± 1.82
σ	2.54 ± 0.06	1.53 ± 0.08	2.55 ± 0.10	1.64 ± 0.12	2.61 ± 0.09	1.42 ± 0.36	2.59 ± 0.10	1.51 ± 0.09

3.4. Texture profile analysis

Texture profile analysis of gels is an important technique for characterising the gel microstructure. In the past TPA has been used to assess how gels perform when it comes to the release of molecules from within their matrices. More rigid, and less elastic gels tends to release molecules slower, owing to a more dense gel network retarding molecular release (Boland, Delahunty, & van Ruth, 2006; Özcan, et al., 2009). While previous studies have carried out TPA on 3DP gels, there exists little, if any, literature that utilises penetration testing, with all the existing work focusing on compression testing (Kamlow, Spyropoulos, et al., 2021; Kamlow, Vadodaria, et al., 2021; Strother, Moss, & McSweeney, 2020; Fanli Yang, Zhang, Bhandari, & Liu, 2018).

Since penetration testing measures force as a function of penetration depth, it is much more sensitive to local variances in the gel architecture. Whereas, compression tests are determined by the average material property for the whole sample (C. M. Lee & Chung, 1989). Penetration testing data for both the 3DP and cast κC-emulsion gels studied here are shown in Fig. 7. Cast κC-emulsion gels display a typical shaped TPA curve, with one failure point (Fig. 7A), whereas 3DP gels had several peaks and troughs, with each of these roughly corresponding to a penetration depth of 1.2 mm (Fig. 7B); this is also compatible with the printed layer height. The data in Fig. 7 also shows (for both cast and 3DP κC-emulsion gels) that as the concentration of SFO increases, the amount of force required to penetrate the gels decreased. Literature suggests this behaviour to be a result of the oil droplets within the network acting as non-interacting filler particles, with therefore further increases to their population (higher SFO content) resulting in a more pronounced disruption in the formation of the gel network around them, and thus weaker gels (D. Julian Mcclements, et al., 1993).

A previous study by the present authors (Kamlow, Spyropoulos, et al., 2021) revealed no statistically significant difference in the performance of 3DP κC-emulsion gels when undergoing compression tests, regardless of SFO concentration. It was observed that under compression, 3DP gels undergo delamination, breaking down at the semi-fused sites that follow the lines of the printing, as opposed to cast gels which are one continuous network. However, the data for the penetration testing in Fig. 7 highlights that penetration testing can demonstrate a difference in performance for 3DP gels; not only was a difference observed with SFO concentration, but also as a function of the emulsifier chosen. The disparity in the results between compression and penetration testing is due to how failure propagates when gels are subjected to either type of forces. While compression testing evaluates the cohesiveness of the gels, that is to say their overall binding, penetration testing assesses the degree of compactness in the gels, that is to say, their density (C. M. Lee, et al., 1989).

From the force-distance graphs in Fig. 7A and 7B, data for force at break, in g, firmness, in g/mm, and gel strength, in g x mm, could be determined and these are shown in Fig. 7C-E. The 5% SFO cast gels had far higher values for force at break and gel strength because they lacked the extensive network disruption caused by either a high concentration of SFO or the discontinuous nature of a 3DP bulk structure. This was responsible for the far higher values observed in Fig. 7C and 7D for 5% SFO cast gels. In terms of force at break and gel strength (Fig. 7C and D), there was a statistically significant difference between the emulsion gels stabilised by either T20 or WPI, except for the cast 5% SFO gels. WPI contains 3.16%, milk-based ash contains cations such as potassium and calcium which are known to reinforce κC gels (Hermansson, et al., 1991). It is believed that this was a contributing factor, to the WPI-stabilised emulsion gels requiring more force before failure. The firmness data (Fig. 7E) saw the 5% SFO gels having no significant difference between them, regardless of emulsifier. For the 40% SFO cast gels, there was no significant difference between the cast gels stabilised by WPI, and the 5% SFO gels. While the 40% SFO cast gels stabilised by T20 were statistically significantly different from the 5% SFO gels, but not the 40% SFO cast gel stabilised by WPI. Between the 40% SFO 3DP gels there was no statistically significant difference, nor was there one with the 40% SFO cast emulsion gel stabilised by T20, but there was for the 40% SFO

cast gel stabilised by WPI. The lower firmness values of the 40% SFO gels, both cast and 3DP, suggest that these systems deformed more easily and tended to flow more before breaking, when compared to the 5% SFO gels (Pang, Deeth, Sopade, Sharma, & Bansal, 2014).

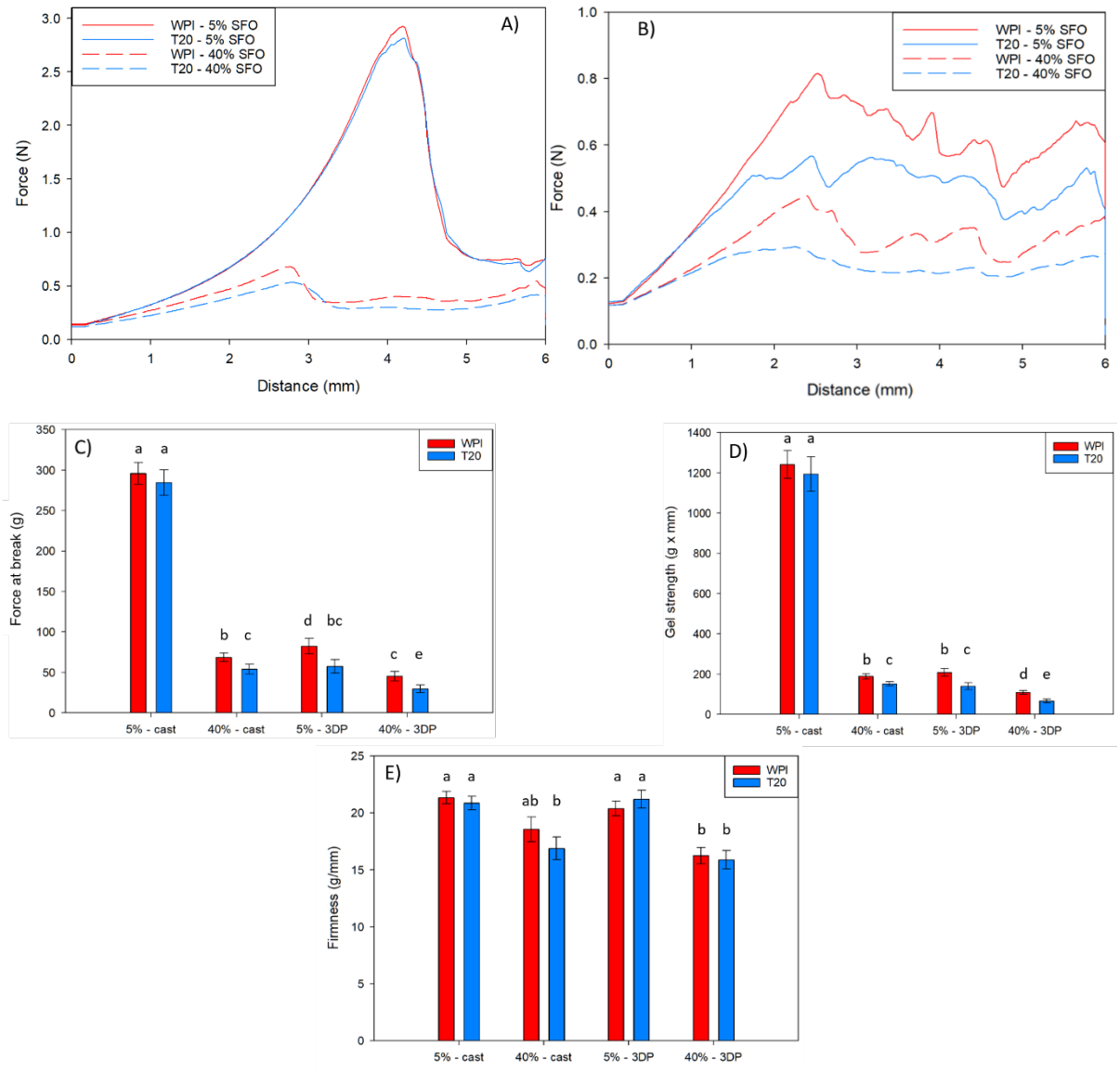

Figure 7: Force-time graphs for (A) cast and (B) 3DP κC-emulsion gels stabilised by T20 and WPI. (C) Force at break, (D) Gel strength and (E) Firmness of the 3DP and cast κC emulsion gel cuboids containing emulsions stabilised by T20 and WPI. Letters represent statistical significance (P<0.05)

3.5. Release studies

The amount of cinnamaldehyde released from 3DP and cast κC-emulsion gels was measured at 37 °C and 20 °C in water as a simple release medium and PBS and 0.1M HCl as they are more physiologically relevant release media. Control cinnamaldehyde release performance from non-gelled emulsions and a pure sunflower oil phase (both) in water at 37 °C, was also assessed. The release data acquired are all presented in Fig 8 and Fig S2.

The release data showed no major difference in the amount of cinnamaldehyde being released from emulsion gels, regardless of whether they were 3DP or cast. This differed from our previous study which found that 3DP gels released a greater proportion of their active in the same timeframe compared to cast gels (Kamlow, Vadodaria, et al., 2021). However, the previous study was for a hydrophilic active directly encased within the gel network, while the present work studies the release of cinnamaldehyde (which is lipophilic) from emulsion gels. This appears to suggest that in the current study, overall cinnamaldehyde release from both the 3DP and cast κC-emulsion gels is predominantly dictated by the active's liberation from the oil droplets rather than by its subsequent discharge from the surrounding gel network. One difference between 3DP and cast gels is observed in Fig. 8A to 8F. Here, there is a divergence in the release performance between the 3DP and cast κC-emulsion gels that is exhibited around the 60-120 mins time frame. Placing the gels into the acceptor medium, creates an osmotic gradient for the transfer of cations from the gel into the aqueous sink; this is controlled by diffusion. This took place at a faster rate in the 3DP (than in the cast) gels, as their inherent layered structure facilitates the migration of the cations into the acceptor phase (Kamlow, Vadodaria, et al., 2021). However, when eventually the gel network of the cast assemblies is also lost, cinnamaldehyde release from these systems is seen to once again coincide with that from their 3DP counterparts. This divergence takes place at later stages in the release experiments utilising PBS as the acceptor phase, owing to the greater concentration of ions (compared to deionised water) present in this case.

In order to confirm that the loss of gelling cations via diffusion causes the collapse of the gels, the data for cinnamaldehyde release in 1M KCl was scrutinised (Fig. S2D). Furthermore cinnamaldehyde release at 20 °C (Fig. S2A-C) was carried out to assess the effect of temperature. In both cases, the previously observed divergence between 3DP and cast κC-emulsion gels was absent, either because the concentration gradient led to the gels taking up salt (1M KCl) or because the lower temperature (20 ºC) has slowed down the diffusional transfer of salts out of the gel network (Vrentas & Vrentas, 1992). This led to release rates being lower in PBS as seen in Fig. 8C-D compared to 19A-B. In 0.1M HCl (Fig. 8E and 8F), a statistically significant increase in the percentage release of cinnamaldehyde was observed. This was due to the free carbonyl group present on cinnamaldehyde, facilitating the formation of Schiff base adducts with an increased aqueous solubility (Friedman, 2017; Wei, Xiong, Jiang, Zhang, & Wen, 2011). In terms of cinnamaldehyde release in an acidic environment (0.1M HCl), WPI stabilised emulsion gel systems behaved differently to those stabilised by T20. As the pH in this case is below the isoelectric point of WPI, the protein has an overall positive charge (Chanamai & McClements, 2002), and thus can associate with κC, effectively acting as a gelling cation (de Kruif, Weinbreck, & de Vries, 2004; Stone & Nickerson, 2012). This meant that the cast and 3DP gels remained solid, despite any potential loss of gelling cations such as potassium and sodium to the acceptor phase. This yielded the different release behaviour compared to the remaining release studies at 37 ˚C. The enhanced aqueous solubility of cinnamaldehyde within an acidic environment can be seen through comparison of Fig. 8E and 8F with Fig. 8A-D, with the release in 0.1M HCl yielding a statistically significant increased amount of cinnamaldehyde compared to release in other media; this trend persists at 20 ˚C as well as shown in the supplementary information. This shows that simply by controlling the emulsifier used to stabilise the κC-emulsion gels, the release rate of active molecules can be manipulated based on the release medium. The enhanced solubility and release of cinnamaldehyde in 0.1M HCl compared to water, was also observed when the active was simply delivered by dissolution in a pure SFO phase, as seen in Fig. S2F. Here there was again, a statistically significant difference in release based on the release medium tested (0.1M HCl or water).

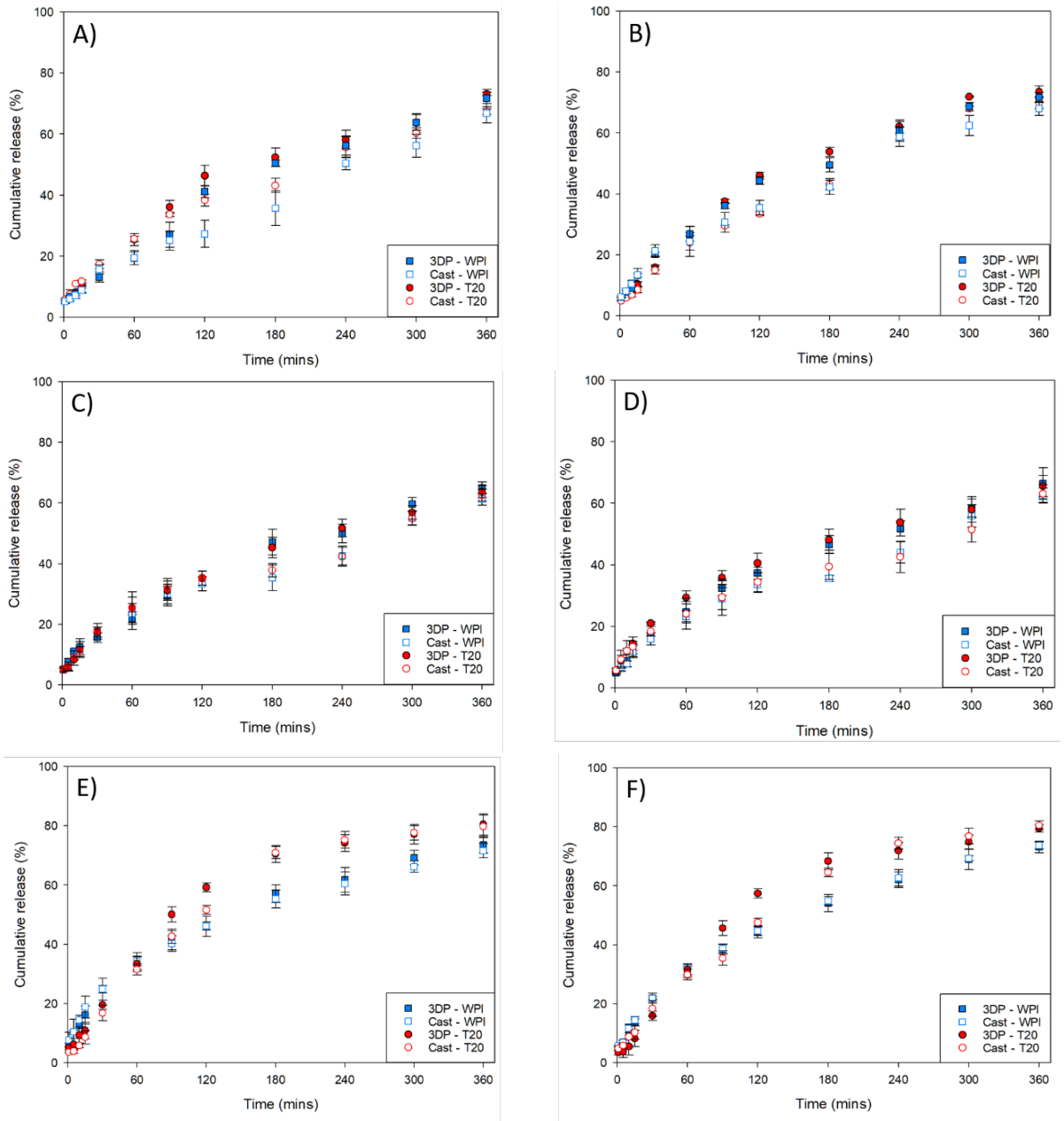

Figure 8: A comparison of cumulative release rates of cinnamaldehyde from 3DP and cast κC-emulsion gels at 37 ˚C in water stabilised by T20 and WPI in the (A) micron and (B) sub-micron scale and the same order is followed for the remaining figures with (C-D) in PBS, (E-F) in 0.1M HCl

Another observation was that there was no significant difference in the trends for final release concentrations observed between the micron and sub-micron scale emulsions gels, and this held true even for the simple emulsion systems in Fig. S2E. Even though a smaller average droplet size yields an increased surface (interfacial) area, that should accelerate release out of the oil globules, literature in this area includes a number of conflicting results (Li & McClements, 2010). Some studies have reported that such a droplet size reduction yields an increase in percentage release of lipophilic molecules (Charles, Lambert, Brondeur, Courthaudon, & Guichard, 2000; S. J. Lee & McClements, 2010), whereas others suggest that droplet size variations have no significant difference (Ahmed, Li, McClements, & Xiao, 2012). Additionally, the use of dialysis tubing has been shown to act as a rate limiting step for the release of lipophiles from emulsion systems, and this may have contributed in not observing

a statistically significant difference between the micron and sub-micron scale systems (Magalhaes, Cave, Seiller, & Benita, 1991). Finally, the possibility exists that κC and cinnamaldehyde interactions via hydrogen bonding could have impeded the release of the active from the gels (Yamada & Shizuma, 2021). The final cinnamaldehyde release values for the release data are presented in Table 2.

Table 2: Final cinnamaldehyde release values as a %. Superscript letters indicate statistical significance (P<0.05)

Cinnamaldehyde-carrying system	**Acceptor Phase**	**Temp. (ºC)**	**Cinnamaldehyde cumulative release (%) after 6 hours**							
pure SFO phase	Water	37	82.9[a]							
	0.1M HCl	37	89.3[b]							
			Micron				**Sub-micron**			
			T20		**WPI**		**T20**		**WPI**	
O/W emulsion	Water	37	76.8[c]		76.3[c]		77.7[c]		77.8[c]	
			3DP	**Cast**	**3DP**	**Cast**	**3DP**	**Cast**	**3DP**	**Cast**
O/W emulsion gel	Water	37	71.2[d]	68.4[d]	71.4[d]	68.8[d]	71.5[d]	69.9[d]	71.7[d]	69.0[d]
		20	55.6[e]	58.3[e]	56.2[e]	60.1[e]	-	-	-	-
	PBS	37	63.7[f]	62.6[f]	65.0[f]	61.2[f]	64.6[f]	63.1[f]	64.4[f]	62.6[f]
		20	53.1[g]	53.5[g]	51.9[g]	52.2[g]	-	-	-	-
	0.1M HCl	37	80.5[h]	79.8[h]	74.6[l]	74.6[l]	79.5[h]	80.5[h]	74.2[l]	74.7[l]
		20	66.4[f]	69.4[df]	66.0[f]	66.2[f]	-	-	-	-
	1M KCl	37	65.1[f]	67.5[f]	63.6[f]	64.5[f]	-	-	-	-
*O/W emulsion gel**	Water	37	69.3[d]	69.1[d]	68.8[d]	68.7[d]	-	-	-	-

*****This system was used for the co-release of cinnamaldehyde (cinn; enclosed within the oil droplets of the O/W emulsion gels) and erioglaucine disodium salt (EDS; entrapped within the gel network of the O/W emulsion gels)

The co-release profiles for cinnamaldehyde and EDS from both the printed and cast κC-emulsion gels and for all release media, were fitted to Ritger-Peppas model shown in Eq [3] in order to assess the contributions of diffusion and relaxation to the release of the active molecules (Ritger, et al., 1987). The exponent m values resulting from the fits are given in Table 3. The data suggests cinnamaldehyde release from 3DP cylinders is driven primarily by Fickian diffusion as opposed to relaxation of the polymer chains. This is believed to be due to the differences in the internal bulk structures of the 3DP cylinders allowing water to penetrate faster into the 3DP shapes compared to cast gel structures. This leads to a greater diffusion contribution to release compared to the relaxational contribution (Falk, Garramone, & Shivkumar, 2004; Kamlow, Vadodaria, et al., 2021). This is demonstrated by the cast gels having m values further away from 0.5, indicating that the relaxational contribution is amplified. This supports the notion that water was unable to penetrate into the cast cylinders as quickly as the 3DP cylinders, meaning that the relaxation of the polymer chains played a bigger part in the release of the actives.

This modelling data further supports some of the previous conclusions made about differences in release of cinnamaldehyde from micron and sub-micron scale oil droplets. The different droplet length scales did not see a significant difference in cinnamaldehyde release with regards to diffusion and relaxational contributions. The release tests carried in 0.1M HCl, showed that the WPI had a larger relaxational contribution, most likely due to the fact that the network remained intact owing to the WPI molecules stabilising the κC-gel network. The release tests carried out at 20 ˚C had larger m values owing to the decreased energy in the system, slowing the diffusion contribution, and this meant that there was as delay as relaxation

had to come into effect to drive more of the release. In terms of the co-release experiments, the presence of the EDS releasing had no effect on the observed release phenomena of the cinnamaldehyde. This provides further evidence that their release occurred through two different mechanisms. The m values for EDS release were higher for the cast gels, compared to the 3DP gels. While our previous study highlighted a much starker difference between 3DP and cast gels for release of a hydrophilic molecule, there were differences such as the lack of dialysis tubing and the previous active, vitamin B1 being cationic, meaning it complexed with the κC which would have affected its release rate (Kamlow, Vadodaria, et al., 2021). 1M KCl did not have a significant effect on the m value compared to the other release media, showing that the gels turning to liquid did not necessarily affect the contributions of diffusion and relaxation to the release. This is highlighted by the similar values observed with the simple emulsions. This further supports the release of the cinnamaldehyde primarily occurring because of expulsion from the oil droplets, rather than the gel network itself.

Table 3: Data on the exponent m, which indicates the balance between the relaxational and diffusional contribution to the release of cinnamaldehyde and EDS.

Active-carrying system	Acceptor Phase	Temp (ºC)	Exponent m±SD (R^2)							
			Micron				Submicron			
			T20		WPI		T20		WPI	
O/W emulsion	Water	37	0.55±0.04 (0.99)		0.57±0.04 (0.99)		0.52±0.05 (0.97)		0.51±0.04 (0.98)	
			3DP	**Cast**	**3DP**	**Cast**	**3DP**	**Cast**	**3DP**	**Cast**
O/W emulsion gel	Water	37	0.58±0.03 (0.98)	0.66±0.03 (0.99)	0.58±0.06 (0.98)	0.69±0.03 (0.98)	0.55±0.04 (0.99)	0.65±0.04 (0.99)	0.53±0.03 (0.99)	0.67±0.04 (0.97)
		20	0.65±0.02 (0.99)	0.78±0.02 (0.99)	0.66±0.02 (0.99)	0.72±0.02 (0.99)	-	-	-	-
	PBS	37	0.53±0.02 (0.99)	0.67±0.03 (0.98)	0.55±0.03 (0.99)	0.69±0.03 (0.98)	0.55±0.03 (0.99)	0.67±0.03 (0.98)	0.62±0.01 (0.99)	0.62±0.03 (0.98)
		20	0.72±0.01 (0.99)	0.74±0.02 (0.99)	0.70±0.01 (0.99)	0.73±0.02 (0.99)	-	-	-	-
	0.1M HCl	37	0.58±0.04 (0.99)	0.61±0.04 (0.99)	0.63±0.01 0.99)	0.66±0.01 (0.99)	0.51±0.01 (0.99)	0.59±0.04 (0.99)	0.63±0.02 (0.99)	0.66±0.02 (0.99)
		20	0.62±0.02 (0.99)	0.65±0.02 (0.99)	0.71±0.01 (0.99)	0.75±0.02 (0.99)	-	-	-	-
	1M KCl	37	0.59±0.02 (0.99)	0.68±0.02 (0.99)	0.58±0.02 (0.99)	0.64±0.02 (0.99)	-	-	-	-
*O/W emulsion gel**	Water (cinn.)	37	0.56±0.02 (0.98)	0.69±0.03 (0.98)	0.56±0.03 (0.98)	0.67±0.04 (0.97)	-	-	-	-
	Water (EDS)	37	0.55±0.02 (0.96)	0.62±0.02 (0.98)	0.52±0.03 (0.98)	0.59±0.03 (0.98)	-	-	-	-

*****This system was used for the co-release of cinnamaldehyde (cinn; enclosed within the oil droplets of the O/W emulsion gels) and erioglaucine disodium salt (EDS; entrapped within the gel network of the O/W emulsion gels)

3.6 Co-release study

Co-release κC-emulsion gels was also evaluated. Two actives were introduced within the κC-emulsion gels, with cinnamaldehyde being present within the lipid phase (oil droplets) of the emulsion gels, and EDS entrapped within the aqueous gel phase. This was carried out to assess whether co-release of actives placed within separate compartments of the κC-emulsion gel microstructure can effectively be utilised to enable their independent co-delivery. This approach is certainly unique in the 3DP emulsion gel literature, and thus extends the current capabilities of these systems to also provide opportunities for the design of novel and/or customisable co-release profiles of both hydrophilic and hydrophobic actives. The

release behaviour of the κC-EDS-cinnamaldehyde emulsion gels in water at 37 ˚C were studied and the obtained data is shown in Fig. 9.

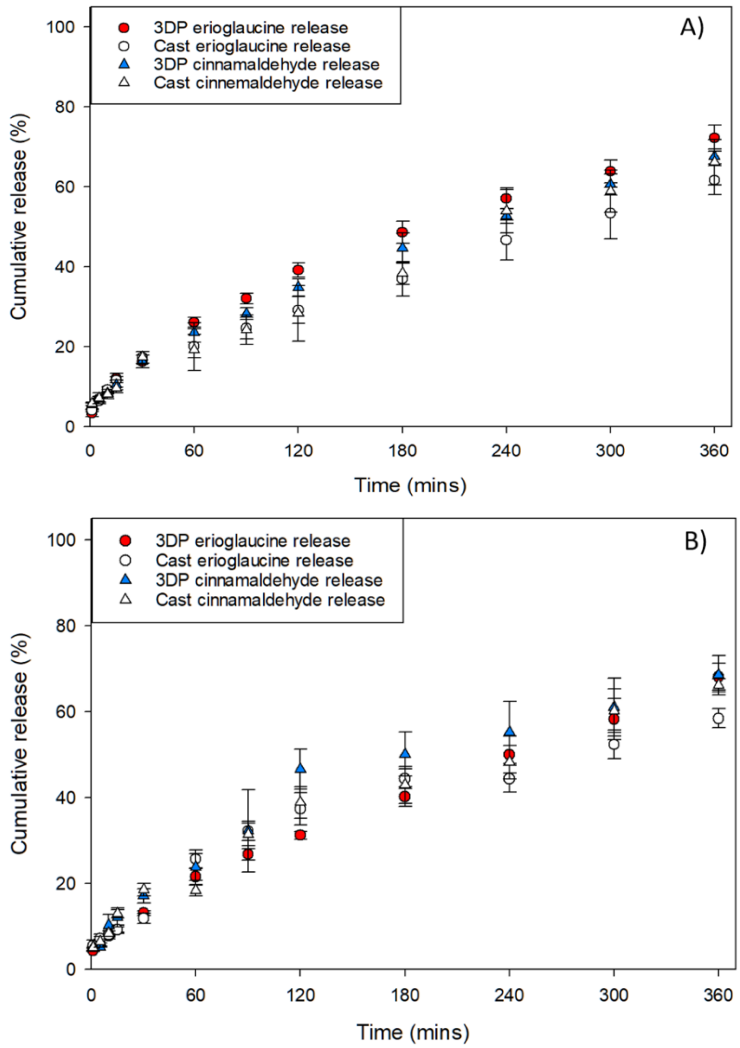

Figure 9: Co-release profiles for cinnamaldehyde and EDS from κC-emulsion gels stabilised by (A) T20 and (B) WPI in water at 37 ˚C.

The release profiles showed no significant difference between T20 and WPI stabilised κC-emulsion gels for the co-release of cinnamaldehyde and EDS. Furthermore, there was once again no significant difference in the final release percentages for the cinnamaldehyde, and the divergence and subsequent convergence could be once more be observed. With the EDS however, there was a statistically significant difference between its release between cast and 3DP gels after 6 hours. This indicates that the release profiles of the two model actives are independently controlled; cinnamaldehyde release is principally controlled by expulsion from the entrapped oil droplets, while EDS release is dictated by the rate of its liberation from the gel network. This is in agreement with previous studies comparing 3DP to cast κC gels when releasing a hydrophilic molecule (Kamlow, Vadodaria, et al., 2021). It should be noted, however, that after 24 hours 100% of the EDS had been released from the gel matrices for both cast and 3DP gels. Compared to the 'mono' release of cinnamaldehyde in water at 37 ˚C, the presence of EDS in the co-release formulation did not have any significant effect on the release of the former active from the κC-emulsion gels. Overall, the data presented here

offer clear confirmation that both 3DP and cast κC-emulsion gels can indeed facilitate the independent co-release of one model lipophilic active (cinnamaldehyde) and one model hydrophilic active (EDS). What is further highlighted here is that the desirable individual co-release profiles can be designed separately and then effectively assembled into one 3DP emulsion gel microstructure, without loss of individual release identity/performance, while utilising 3DP's ability to readily alter the size and shape of the desired product, delivering flexible dosing, without the need of additional moulds or tooling that would be required with cast samples.

4. Conclusions

This study provides further insight into the stability, mechanical and performance characteristics of κC-emulsion gels. 3DP κC-emulsion gels lose slightly more water over time than cast gels, but the 3DP process has no effect on droplet size stability during production or storage of κC-emulsion gels. This study has for the first time highlighted differences between 3DP gels based on their SFO concentration and emulsifier type through penetration testing, with lower SFO concentration and the use of WPI as an emulsifier yielding more resistant gels. This study has shown for the first time in release testing, that the release medium has been shown to affect the release rate of lipophilic molecules from cast and 3DP κC- emulsion gels. However, droplet size and production process had no effect on the release rate, although the use of dialysis tubing might have affected this. Finally, co-release of EDS and cinnamaldehyde was carried out, for the first time from a 3DP bulk structure. This shows that 3DP can be used to create customisable κC gels containing hydrophilic and/or lipophilic active molecules, with desired properties tuneable through variances in SFO concentration, shape, emulsifier type and size. Future studies could focus on the addition of a dietarily appropriate protein and carbohydrate concentrations, to give a total food source that can be fortified with active molecules.

Acknowledgements

This work was supported by the Engineering and Physical Sciences Research Council [grant number EP/N024818/1].

References

Ahmed, K., Li, Y., McClements, D. J., & Xiao, H. (2012). Nanoemulsion- and emulsion-based delivery systems for curcumin: Encapsulation and release properties. *Food Chemistry, 132*(2), 799-807.

Ako, K. (2015). Influence of elasticity on the syneresis properties of κ-carrageenan gels. *Carbohydrate Polymers, 115*, 408-414.

Andrews, G. P., Donnelly, L., Jones, D. S., Curran, R. M., Morrow, R. J., Woolfson, A. D., & Malcolm, R. K. (2009). Characterization of the Rheological, Mucoadhesive, and Drug Release Properties of Highly Structured Gel Platforms for Intravaginal Drug Delivery. *Biomacromolecules, 10*(9), 2427-2435.

Balaguer, M. P., Borne, M., Chalier, P., Gontard, N., Morel, M.-H., Peyron, S., Gavara, R., & Hernandez-Munoz, P. (2013). Retention and Release of Cinnamaldehyde from Wheat Protein Matrices. *Biomacromolecules, 14*(5), 1493-1502.

751 Ben Arfa, A., Preziosi-Belloy, L., Chalier, P., & Gontard, N. (2007). Antimicrobial Paper Based on a Soy
752 Protein Isolate or Modified Starch Coating Including Carvacrol and Cinnamaldehyde. *Journal*
753 *of Agricultural and Food Chemistry, 55*(6), 2155-2162.
754 Beverung, C. J., Radke, C. J., & Blanch, H. W. (1999). Protein adsorption at the oil/water interface:
755 characterization of adsorption kinetics by dynamic interfacial tension measurements.
756 *Biophysical Chemistry, 81*(1), 59-80.
757 Boland, A. B., Delahunty, C. M., & van Ruth, S. M. (2006). Influence of the texture of gelatin gels and
758 pectin gels on strawberry flavour release and perception. *Food Chemistry, 96*(3), 452-460.
759 Buchanan, C., & Gardner, L. (2019). Metal 3D printing in construction: A review of methods,
760 research, applications, opportunities and challenges. *Engineering Structures, 180*, 332-348.
761 Chanamai, R., & McClements, D. J. (2002). Comparison of Gum Arabic, Modified Starch, and Whey
762 Protein Isolate as Emulsifiers: Influence of pH, CaCl2 and Temperature. *Journal of Food*
763 *Science, 67*(1), 120-125.
764 Charles, M., Lambert, S., Brondeur, P., Courthaudon, J.-L., & Guichard, E. (2000). Influence of
765 Formulation and Structure of an Oil-in-Water Emulsion on Flavor Release. In *Flavor Release*
766 (Vol. 763, pp. 342-354): American Chemical Society.
767 Chen, H., Lu, Y., Yuan, F., Gao, Y., & Mao, L. (2021). Effect of interfacial compositions on the physical
768 properties of alginate-based emulsion gels and chemical stability of co-encapsulated
769 bioactives. *Food Hydrocolloids, 111*, 106389.
770 Chen, H., Xie, F., Chen, L., & Zheng, B. (2019). Effect of rheological properties of potato, rice and corn
771 starches on their hot-extrusion 3D printing behaviors. *Journal of Food Engineering, 244*, 150-
772 158.
773 Chen, Z., Li, Z., Li, J., Liu, C., Lao, C., Fu, Y., Liu, C., Li, Y., Wang, P., & He, Y. (2019). 3D printing of
774 ceramics: A review. *Journal of the European Ceramic Society, 39*(4), 661-687.
775 Daffner, K., Ong, L., Hanssen, E., Gras, S., & Mills, T. (2021). Characterising the influence of milk fat
776 towards an application for extrusion-based 3D-printing of casein−whey protein suspensions
777 via the pH−temperature-route. *Food Hydrocolloids*, 106642.
778 Daffner, K., Vadodaria, S., Ong, L., Nöbel, S., Gras, S., Norton, I., & Mills, T. (2021). Design and
779 characterization of casein–whey protein suspensions via the pH–temperature-route for
780 application in extrusion-based 3D-Printing. *Food Hydrocolloids, 112*, 105850.
781 de Kruif, C. G., Weinbreck, F., & de Vries, R. (2004). Complex coacervation of proteins and anionic
782 polysaccharides. *Current Opinion in Colloid & Interface Science, 9*(5), 340-349.
783 Diañez, I., Gallegos, C., Brito-de la Fuente, E., Martínez, I., Valencia, C., Sánchez, M. C., Diaz, M. J., &
784 Franco, J. M. (2019). 3D printing in situ gelification of κ-carrageenan solutions: Effect of
785 printing variables on the rheological response. *Food Hydrocolloids, 87*, 321-330.
786 Falk, B., Garramone, S., & Shivkumar, S. (2004). Diffusion coefficient of paracetamol in a chitosan
787 hydrogel. *Materials Letters, 58*(26), 3261-3265.
788 Fenton, T., Gholamipour-Shirazi, A., Daffner, K., Mills, T., & Pelan, E. (2021). Formulation and
789 additive manufacturing of polysaccharide-surfactant hybrid gels as gelatin analogues in food
790 applications. *Food Hydrocolloids, 120*, 106881.
791 Fiszman, S. M., Lluch, M. A., & Salvador, A. (1999). Effect of addition of gelatin on microstructure of
792 acidic milk gels and yoghurt and on their rheological properties. *International Dairy Journal,*
793 *9*(12), 895-901.
794 Fiszman, S. M., & Salvador, A. (1999). Effect of gelatine on the texture of yoghurt and of acid-heat-
795 induced milk gels. *Zeitschrift für Lebensmitteluntersuchung und -Forschung A, 208*(2), 100-
796 105.
797 Friedman, M. (2017). Chemistry, Antimicrobial Mechanisms, and Antibiotic Activities of
798 Cinnamaldehyde against Pathogenic Bacteria in Animal Feeds and Human Foods. *Journal of*
799 *Agricultural and Food Chemistry, 65*(48), 10406-10423.
800 Gholamipour-Shirazi, A., Kamlow, M.-A., T Norton, I., & Mills, T. (2020). How to formulate for
801 structure and texture via medium of additive manufacturing-a review. *Foods, 9*(4), 497.

Gholamipour-Shirazi, A., Norton, I. T., & Mills, T. (2019). Designing hydrocolloid based food-ink formulations for extrusion 3D printing. *Food Hydrocolloids, 95*, 161-167.
Gholamipour-Shirazi, A., Norton, I. T., & Mills, T. (2021). Dual stimuli-sensitive carrageenan-based formulation for additive manufacturing. *International Journal of Biological Macromolecules, 189*, 370-379.
Gill, A. O., & Holley, R. A. (2004). Mechanisms of bactericidal action of cinnamaldehyde against Listeria monocytogenes and of eugenol against L. monocytogenes and Lactobacillus sakei. *Applied and environmental microbiology, 70*(10), 5750-5755.
Goudappel, G. J. W., van Duynhoven, J. P. M., & Mooren, M. M. W. (2001). Measurement of Oil Droplet Size Distributions in Food Oil/Water Emulsions by Time Domain Pulsed Field Gradient NMR. *Journal of Colloid and Interface Science, 239*(2), 535-542.
Govindaraj, P., Subramanian, S., & Raghavachari, D. (2021). Preparation of gels of chitosan through a hydrothermal reaction in the presence of malonic acid and cinnamaldehyde: characterization and antibacterial activity. *New Journal of Chemistry, 45*(47), 22101-22112.
Gowder, S. J., & Devaraj, H. (2006). Effect of the food flavour cinnamaldehyde on the antioxidant status of rat kidney. *Basic & clinical pharmacology & toxicology, 99*(5), 379-382.
Goyanes, A., Scarpa, M., Kamlow, M., Gaisford, S., Basit, A. W., & Orlu, M. (2017). Patient acceptability of 3D printed medicines. *Int J Pharm, 530*(1-2), 71-78.
Hermansson, A.-M., Eriksson, E., & Jordansson, E. (1991). Effects of potassium, sodium and calcium on the microstructure and rheological behaviour of kappa-carrageenan gels. *Carbohydrate Polymers, 16*(3), 297-320.
Hu, Y., Wang, J., Li, X., Hu, X., Zhou, W., Dong, X., Wang, C., Yang, Z., & Binks, B. P. (2019). Facile preparation of bioactive nanoparticle/poly(ε-caprolactone) hierarchical porous scaffolds via 3D printing of high internal phase Pickering emulsions. *Journal of Colloid and Interface Science, 545*, 104-115.
Jeong, H.-S., Kim, E., Nam, C., Choi, Y., Lee, Y.-J., Weitz, D. A., Lee, H., & Choi, C.-H. (2021). Hydrogel Microcapsules with a Thin Oil Layer: Smart Triggered Release via Diverse Stimuli. *Advanced Functional Materials, 31*(18), 2009553.
Jin, Y., Compaan, A., Bhattacharjee, T., & Huang, Y. (2016). Granular gel support-enabled extrusion of three-dimensional alginate and cellular structures. *Biofabrication, 8*(2), 025016.
Johannesson, J., Khan, J., Hubert, M., Teleki, A., & Bergström, C. A. S. (2021). 3D-printing of solid lipid tablets from emulsion gels. *International Journal of Pharmaceutics, 597*, 120304.
Juslin, L., Antikainen, O., Merkku, P., & Yliruusi, J. (1995). Droplet size measurement: I. Effect of three independent variables on droplet size distribution and spray angle from a pneumatic nozzle. *International Journal of Pharmaceutics, 123*(2), 247-256.
Kamlow, M.-A., Spyropoulos, F., & Mills, T. (2021b). 3D printing of kappa-carrageenan emulsion gels. *Food Hydrocolloids for Health, 1*, 100044.
Kamlow, M.-A., Vadodaria, S., Gholamipour-Shirazi, A., Spyropoulos, F., & Mills, T. (2021). 3D printing of edible hydrogels containing thiamine and their comparison to cast gels. *Food Hydrocolloids, 116*, 106550.
Kenta, S., Raikos, V., Vagena, A., Sevastos, D., Kapolos, J., Koliadima, A., & Karaiskakis, G. (2013). Kinetic study of aggregation of milk protein and/or surfactant-stabilized oil-in-water emulsions by Sedimentation Field-Flow Fractionation. *Journal of Chromatography A, 1305*, 221-229.
Lanaro, M., Desselle, M. R., & Woodruff, M. A. (2019). 3D Printing Chocolate. In *Fundamentals of 3D Food Printing and Applications* (pp. 151-173).
Lee, C. M., & Chung, K. H. (1989). Analysis of surimi gel properties by compression and penetration tests. *Journal of Texture Studies, 20*(3), 363-377.
Lee, S. J., & McClements, D. J. (2010). Fabrication of protein-stabilized nanoemulsions using a combined homogenization and amphiphilic solvent dissolution/evaporation approach. *Food Hydrocolloids, 24*(6), 560-569.

Li, Y., & McClements, D. J. (2010). New Mathematical Model for Interpreting pH-Stat Digestion Profiles: Impact of Lipid Droplet Characteristics on in Vitro Digestibility. *Journal of Agricultural and Food Chemistry, 58*(13), 8085-8092.
Liu, F., & Tang, C.-H. (2016). Soy glycinin as food-grade Pickering stabilizers: Part. III. Fabrication of gel-like emulsions and their potential as sustained-release delivery systems for β-carotene. *Food Hydrocolloids, 56*, 434-444.
Liu, H., Nie, Y., & Chen, H. (2014). Effect of Different Starches on Colors and Textural Properties of Surimi-Starch Gels. *International Journal of Food Properties, 17*(7), 1439-1448.
Liu, Z., Bhandari, B., Prakash, S., Mantihal, S., & Zhang, M. (2019). Linking rheology and printability of a multicomponent gel system of carrageenan-xanthan-starch in extrusion based additive manufacturing. *Food Hydrocolloids, 87*, 413-424.
Lu, B., Tarn, M. D., Pamme, N., & Georgiou, T. K. (2018). Fabrication of tailorable pH responsive cationic amphiphilic microgels on a microfluidic device for drug release. *Journal of Polymer Science Part A: Polymer Chemistry, 56*(1), 59-66.
Magalhaes, N. S. S., Cave, G., Seiller, M., & Benita, S. (1991). The stability and in vitro release kinetics of a clofibride emulsion. *International Journal of Pharmaceutics, 76*(3), 225-237.
Matsumura, Y., Kang, I.-J., Sakamoto, H., Motoki, M., & Mori, T. (1993). Filler effects of oil droplets on the viscoelastic properties of emulsion gels. *Food Hydrocolloids, 7*(3), 227-240.
McClements, D. J. (2018). Enhanced delivery of lipophilic bioactives using emulsions: a review of major factors affecting vitamin, nutraceutical, and lipid bioaccessibility. *Food & function, 9*(1), 22-41.
Mcclements, D. J., Monahan, F. J., & Kinsella, J. E. (1993). Effect Of Emulsion Droplets On The Rheology Of Whey Protein Isolate Gels. *Journal of Texture Studies, 24*(4), 411-422.
Nagula, R. L., & Wairkar, S. (2019). Recent advances in topical delivery of flavonoids: A review. *Journal of Controlled Release, 296*, 190-201.
Norton, I. T., Morris, E. R., & Rees, D. A. (1984). Lyotropic effects of simple anions on the conformation and interactions of kappa-carrageenan. *Carbohydrate research, 134*(1), 89-101.
Özcan, İ., Abacı, Ö., Uztan, A. H., Aksu, B., Boyacıoğlu, H., Güneri, T., & Özer, Ö. (2009). Enhanced topical delivery of terbinafine hydrochloride with chitosan hydrogels. *Aaps Pharmscitech, 10*(3), 1024-1031.
Pal, R., & Rhodes, E. (1989). Viscosity/concentration relationships for emulsions. *Journal of Rheology, 33*(7), 1021-1045.
Pallottino, F., Hakola, L., Costa, C., Antonucci, F., Figorilli, S., Seisto, A., & Menesatti, P. (2016). Printing on food or food printing: a review. *Food and Bioprocess Technology, 9*(5), 725-733.
Pang, Z., Deeth, H., Sopade, P., Sharma, R., & Bansal, N. (2014). Rheology, texture and microstructure of gelatin gels with and without milk proteins. *Food Hydrocolloids, 35*, 484-493.
Phillips, G. O., & Williams, P. A. (2009). *Handbook of hydrocolloids*: Elsevier.
Rahim, T. N. A. T., Abdullah, A. M., & Md Akil, H. (2019). Recent developments in fused deposition modeling-based 3D printing of polymers and their composites. *Polymer Reviews, 59*(4), 589-624.
Ricci, I., Derossi, A., & Severini, C. (2019). 3D Printed Food From Fruits and Vegetables. In *Fundamentals of 3D Food Printing and Applications* (pp. 117-149).
Ritger, P. L., & Peppas, N. A. (1987). A simple equation for description of solute release I. Fickian and non-fickian release from non-swellable devices in the form of slabs, spheres, cylinders or discs. *Journal of Controlled Release, 5*(1), 23-36.
Rostami, H., Nikoo, A. M., Rajabzadeh, G., Niknia, N., & Salehi, S. (2018). Development of cumin essential oil nanoemulsions and its emulsion filled hydrogels. *Food Bioscience, 26*, 126-132.

902 Serizawa, R., Shitara, M., Gong, J., Makino, M., Kabir, M. H., & Furukawa, H. (2014). 3D jet printer of
903 edible gels for food creation. In *Behavior and Mechanics of Multifunctional Materials and*
904 *Composites 2014* (Vol. 9058, pp. 90580A): International Society for Optics and Photonics.
905 Siddiqua, S., Anusha, B., Ashwini, L., & Negi, P. (2015). Antibacterial activity of cinnamaldehyde and
906 clove oil: effect on selected foodborne pathogens in model food systems and watermelon
907 juice. *Journal of food science and technology, 52*(9), 5834-5841.
908 Singh, B., Kaur, T., & Singh, S. (1997). Correction of raw dissolution data for loss of drug and volume
909 during sampling. *Indian journal of pharmaceutical sciences, 59*(4), 196.
910 Singh, H., Tamehana, M., Hemar, Y., & Munro, P. A. (2003). Interfacial compositions, microstructure
911 and stability of oil-in-water emulsions formed with mixtures of milk proteins and κ-
912 carrageenan: 2. Whey protein isolate (WPI). *Food Hydrocolloids, 17*(4), 549-561.
913 Singla, V., Saini, S., Joshi, B., & Rana, A. (2012). Emulgel: A new platform for topical drug delivery.
914 *International Journal of Pharma and Bio Sciences, 3*(1), 485-498.
915 Stone, A. K., & Nickerson, M. T. (2012). Formation and functionality of whey protein isolate–(kappa-,
916 iota-, and lambda-type) carrageenan electrostatic complexes. *Food Hydrocolloids, 27*(2),
917 271-277.
918 Strother, H., Moss, R., & McSweeney, M. B. (2020). Comparison of 3D printed and molded carrots
919 produced with gelatin, guar gum and xanthan gum. *Journal of Texture Studies, 51*(6), 852-
920 860.
921 Sun, J., Zhou, W., Huang, D., Fuh, J. Y. H., Hong, G. S. J. F., & Technology, B. (2015). An Overview of
922 3D Printing Technologies for Food Fabrication. *8*(8), 1605-1615.
923 Teo, A., Goh, K. K. T., Wen, J., Oey, I., Ko, S., Kwak, H.-S., & Lee, S. J. (2016). Physicochemical
924 properties of whey protein, lactoferrin and Tween 20 stabilised nanoemulsions: Effect of
925 temperature, pH and salt. *Food Chemistry, 197*, 297-306.
926 Thakur, G., Naqvi, M. A., Rousseau, D., Pal, K., Mitra, A., & Basak, A. (2012). Gelatin-Based Emulsion
927 Gels for Diffusion-Controlled Release Applications. *Journal of Biomaterials Science, Polymer*
928 *Edition, 23*(5), 645-661.
929 Thrimawithana, T. R., Young, S., Dunstan, D. E., & Alany, R. G. (2010). Texture and rheological
930 characterization of kappa and iota carrageenan in the presence of counter ions.
931 *Carbohydrate Polymers, 82*(1), 69-77.
932 Ubbink, J., Burbidge, A., & Mezzenga, R. (2008). Food structure and functionality: a soft matter
933 perspective. *Soft Matter, 4*(8), 1569-1581.
934 Vadodaria, S. S., He, Y., Mills, T., & Wildman, R. (2020). Fabrication of surfactant-polyelectrolyte
935 complex using valvejet 3D printing-aided colloidal self assembly. *Colloids and Surfaces A:*
936 *Physicochemical and Engineering Aspects, 600*, 124914.
937 van der Ven, C., Gruppen, H., de Bont, D. B. A., & Voragen, A. G. J. (2001). Emulsion Properties of
938 Casein and Whey Protein Hydrolysates and the Relation with Other Hydrolysate
939 Characteristics. *Journal of Agricultural and Food Chemistry, 49*(10), 5005-5012.
940 Vrentas, J., & Vrentas, C. (1992). Fickian diffusion in glassy polymer-solvent systems. *Journal of*
941 *Polymer Science Part B: Polymer Physics, 30*(9), 1005-1011.
942 Wang, J., Gao, H., Hu, Y., Zhang, N., Zhou, W., Wang, C., Binks, B. P., & Yang, Z. (2021). 3D printing of
943 Pickering emulsion inks to construct poly(D,L-lactide-co-trimethylene carbonate)-based
944 porous bioactive scaffolds with shape memory effect. *Journal of Materials Science, 56*(1),
945 731-745.
946 Wei, Q.-Y., Xiong, J.-J., Jiang, H., Zhang, C., & Wen, Y. (2011). The antimicrobial activities of the
947 cinnamaldehyde adducts with amino acids. *International Journal of Food Microbiology,*
948 *150*(2), 164-170.
949 Wiącek, A., & Chibowski, E. (1999). Zeta potential, effective diameter and multimodal size
950 distribution in oil/water emulsion. *Colloids and Surfaces A: Physicochemical and Engineering*
951 *Aspects, 159*(2), 253-261.

952 Wiącek, A. E., & Chibowski, E. (2002). Zeta potential and droplet size of n-tetradecane/ethanol
953 (protein) emulsions. *Colloids and Surfaces B: Biointerfaces, 25*(1), 55-67.
954 Wu, Y., Petrochenko, P., Chen, L., Wong, S. Y., Absar, M., Choi, S., & Zheng, J. (2016). Core size
955 determination and structural characterization of intravenous iron complexes by cryogenic
956 transmission electron microscopy. *International Journal of Pharmaceutics, 505*(1), 167-174.
957 Yamada, Y., & Shizuma, M. (2021). Study on release suppression of cinnamaldehyde from κ-
958 carrageenan gel by HR-MASNMR and pulsed field gradient NMR (PFG-NMR). *Food*
959 *Hydrocolloids, 110*, 106130.
960 Yang, F., Zhang, M., Bhandari, B., & Liu, Y. (2018). Investigation on lemon juice gel as food material
961 for 3D printing and optimization of printing parameters. *Lwt, 87*, 67-76.
962 Yang, F., Zhang, M., Prakash, S., & Liu, Y. (2018). Physical properties of 3D printed baking dough as
963 affected by different compositions. *Innovative Food Science & Emerging Technologies, 49*,
964 202-210.
965 Zhang, L., Zheng, J., Wang, Y., Ye, X., Chen, S., Pan, H., & Chen, J. (2022). Fabrication of
966 rhamnogalacturonan-I enriched pectin-based emulsion gels for protection and sustained
967 release of curcumin. *Food Hydrocolloids, 128*, 107592.

968

SUPPLAMENTARY INFORMATION

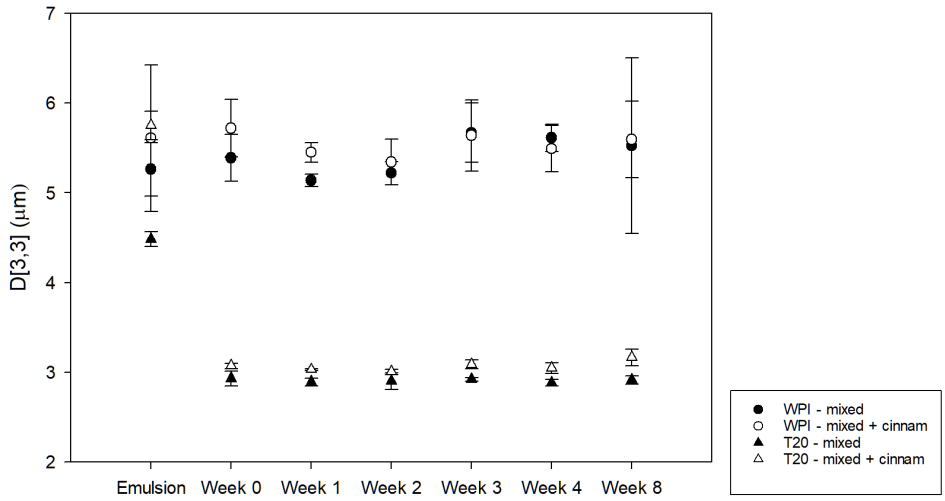

Figure S1: TD-NMR over 8 weeks showing D3,3 values for κC-emulsion gels containing mixed micron and sub-micron scale emulsions with and without cinnamaldehyde

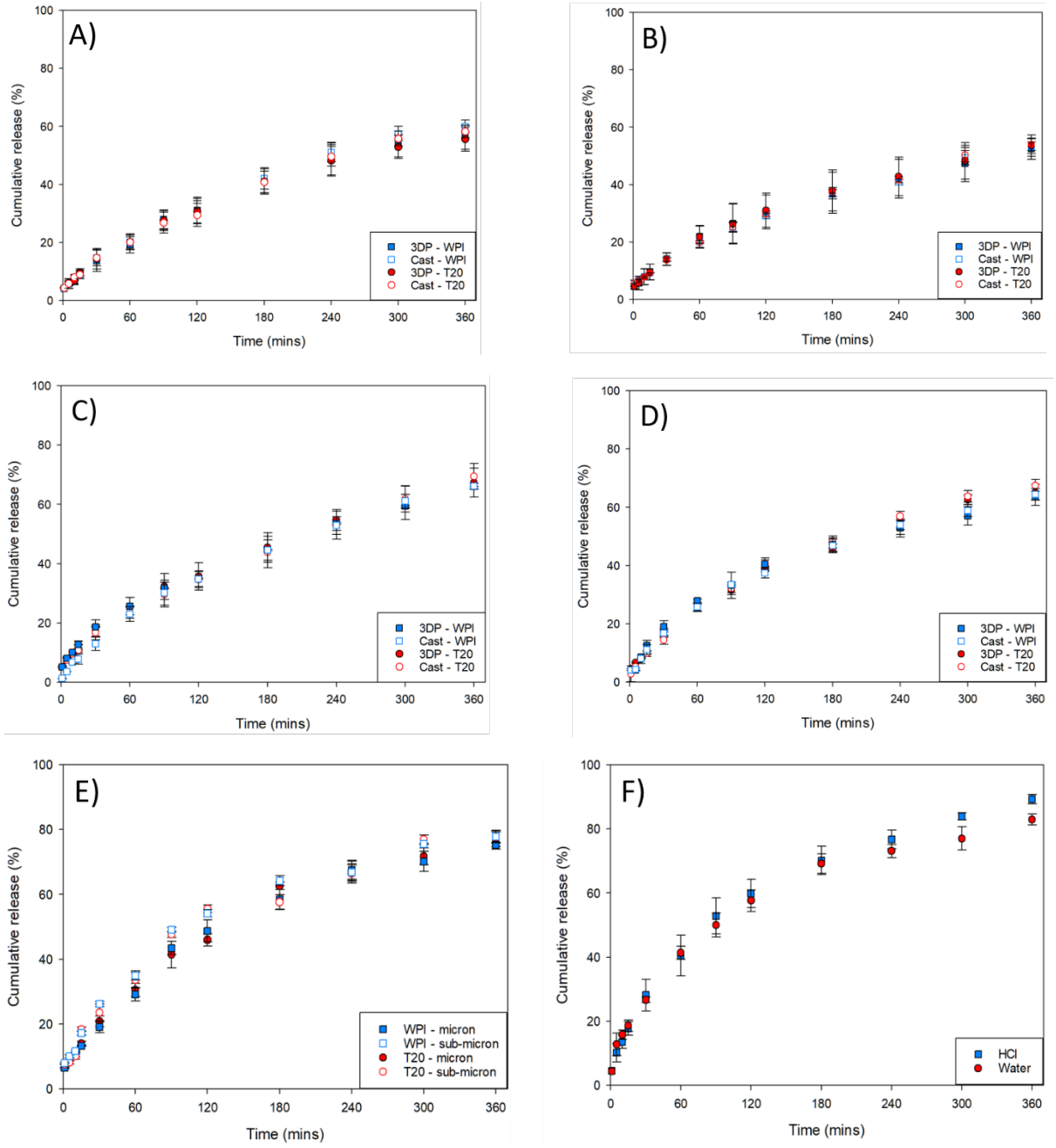

Figure S2: A comparison of cumulative release rates of cinnamaldehyde from 3DP and cast κC-emulsion gels stabilised by T20 or WPI, at (A) 20 ˚C in water (B) PBS at 20 ˚C, (C) 0.1M HCl at 20 ˚C, (D) 1M KCl at 37 ˚C, (E) release from non-gelled emulsions in water at 37 ˚C and (F) release from cinnamaldehyde mixed with SFO in HCl and water at 37 ˚C